Preference-Driven Multi-Objective Combinatorial Optimization with Conditional Computation

Mingfeng Fan

National University of Singapore ming.fan@nus.edu.sg

Yifeng Zhang

National University of Singapore yifeng@u.nus.edu

Jinbiao Chen

Sun Yat-sen University chenjb69@mail2.sysu.edu.cn

Jianan Zhou*

Nanyang Technological University jianan004@e.ntu.edu.sg

Yaoxin Wu*

Eindhoven University of Technology y.wu2@tue.nl

Guillaume Adrien Sartoretti

National University of Singapore guillaume.sartoretti@nus.edu.sg

Abstract

Recent deep reinforcement learning methods have achieved remarkable success in solving multi-objective combinatorial optimization problems (MOCOPs) by decomposing them into multiple subproblems, each associated with a specific weight vector. However, these methods typically treat all subproblems equally and solve them using a single model, hindering the effective exploration of the solution space and thus leading to suboptimal performance. To overcome the limitation, we propose POCCO, a novel plug-and-play framework that enables adaptive selection of model structures for subproblems, which are subsequently optimized based on preference signals rather than explicit reward values. Specifically, we design a conditional computation block that routes subproblems to specialized neural architectures. Moreover, we propose a preference-driven optimization algorithm that learns pairwise preferences between winning and losing solutions. We evaluate the efficacy and versatility of POCCO by applying it to two state-of-the-art neural methods for MOCOPs. Experimental results across four classic MOCOP benchmarks demonstrate its significant superiority and strong generalization.

1 Introduction

Multi-objective combinatorial optimization problems (MOCOPs) involve optimizing multiple conflicting objectives within a discrete decision space. They have attracted considerable attention from the computer science and operations research communities due to their widespread applications in manufacturing [1], logistics [25], and scheduling [17]. In such scenarios, decision makers must simultaneously consider and balance multiple criteria, such as cost, makespan, and environmental impact. Unlike single-objective combinatorial optimization problems (SOCOPs), which seek a single optimal solution, MOCOPs aim to identify Pareto optimal solutions that reflect trade-offs among conflicting objectives, making them inherently more challenging. Given their NP-hard nature, exact methods typically struggle to solve MOCOPs within reasonable time frames, as computational complexity may increase exponentially with problem scale [13, 16]. Consequently, heuristic approaches have emerged as the main avenue for tackling MOCOPs. However, these heuristics often involve extensive iterative

^{*}Corresponding author.

local searches for each new instance, resulting in high computational costs. Furthermore, conventional heuristics often rely on extensive domain-specific expertise and meticulous, problem-specific tuning, thus limiting their adaptability to broader classes of MOCOPs.

Recently, neural methods have achieved great success in solving SOCOPs [3, 8, 22, 27, 33, 43, 60, 69, 70] by learning effective patterns of decision policies in a data-driven way. Motivated by these advances, researchers have extended neural approaches to MOCOPs, leveraging their advantages in bypassing labor-intensive heuristic design, accelerating problem solving through GPU parallelization, and flexibly adapting to diverse MOCOP variants. Typically, neural methods address MOCOPs by decomposing them into a set of scalarized subproblems, each a SOCOP defined by a specific weight vector, and solving them using deep reinforcement learning (DRL) to approximate the Pareto front. Early approaches train or fine-tune a separate model for each subproblem using transfer learning or meta-learning techniques [34, 67]. However, these approaches require extensive computational resources and struggle to generalize to subproblems with unseen weight vectors. As an alternative, PMOCO [38] employs a weight-conditioned hypernetwork to modulate model parameters, allowing a single model to address all subproblems. Nevertheless, it remains limited in effectively handling subproblems with diverse weight vectors. More recently, methods such as CNH [14] and WE-CA [6] have tackled this challenge by encoding weight vectors directly into the problem representations, resulting in a unified model that generalizes across various problem sizes. These methods are currently considered state-of-the-art (SOTA) in solving MOCOPs.

Current SOTA methods typically rely on a single neural network with limited capacity to handle all subproblems, which overcomplicates the learning task and results in suboptimal performance. A straightforward solution to ease training and promote effective representation learning across subproblems is to increase the model capacity. However, determining *how much* additional capacity to allocate and *where* to introduce it within the architecture remains an open challenge. On the other hand, neural methods often adopt REINFORCE [56] as the training algorithm, relying solely on scalarized objective values as reward signals to guide policy updates. Given its on-policy nature, REINFORCE suffers from high gradient variance and lacks structured mechanisms for effective exploration [32]. These issues are exacerbated in MOCOP settings, where the vast combinatorial action space makes efficient exploration particularly difficult, ultimately hindering policy performance.

To address these issues, we propose POCCO (Preference-driven multi-objective combinatorial Optimization with Conditional COmputation), a plug-and-play framework that augments neural MOCOP methods with two complementary mechanisms. First, POCCO introduces a conditional computation block into the decoder, where a sparse gating network dynamically routes each subproblem through either a selected subset of feed-forward (FF) experts or a parameter-free identity (ID) expert. This design enables subproblems to adaptively select computation routes (i.e., model structures) based on their context, efficiently scaling model capacity and facilitating more effective representation learning. Second, POCCO replaces raw scalarized rewards with pairwise preference learning. For each subproblem, the policy samples two trajectories, identifies the better one as the winner, and maximizes a Bradley–Terry (BT) likelihood based on the difference in their average log-likelihoods. Such comparative feedback guides the search toward policies that generate increasingly preferred solutions, enabling exploration of the most promising regions of the search space and more efficient convergence to higher-quality solutions. Our contributions are summarized as follows:

- Conceptually, we address two fundamental limitations of existing approaches for solving MOCOPs: limited exploration within the vast solution space and the reliance on a single, capacity-limited model, which can lead to inefficient learning and suboptimal performance.
- Technically, we propose a conditional computation block that dynamically routes subproblems to tailored neural architectures. Additionally, we develop a preference-driven algorithm leveraging implicit rewards derived from pairwise preference signals between winning and losing solutions, modeled using the BT framework.
- Experimentally, we demonstrate the effectiveness and versatility of POCCO on classical MOCOP benchmarks using two SOTA neural methods. Extensive results show that POCCO not only outperforms all baseline methods but also exhibits superior generalization across diverse problem sizes.

2 Related Works

Traditional methods for MOCOP. MOCOPs are significantly harder to solve than their single-objective counterparts. Classic cases such as the Traveling Salesman Problem (TSP) and Capacitated Vehicle Routing Problem (CVRP) are already NP-hard, and adding multiple objectives only magnifies the difficulty [16]. Exact algorithms quickly become impractical for large instances or for problems that possess a vast Pareto set [18, 59]. Consequently, research has shifted toward heuristic methods that deliver high-quality Pareto fronts within reasonable time limits [25, 64]. Among these, multi-objective evolutionary algorithms (MOEAs) are widely used. They fall into two main categories: dominance-based MOEAs [11, 12, 46] and decomposition-based MOEAs [15, 26, 65]. Despite their popularity, MOEAs typically demand extensive manual design: practitioners must select and tune crossover, mutation, and selection operators along with many hyperparameters [50, 61, 63], and this labor-intensive hand-engineering often limits overall performance.

Neural methods for MOCOP. Inspired by the success of DRL in SOCOPs [4], recent research extends neural methods to MOCOPs by solving a series of scalarized SOCOPs. These neural solvers generally follow two paradigms: *one-to-one* and *one-to-many*. The one-to-one paradigm trains or fine-tunes a separate neural model for each scalarized subproblem. Some approaches apply DRL algorithms individually and transfer parameters across models to accelerate convergence [34, 57]. Others adopt architectures such as Pointer Networks [52] and Attention Models [29, 30], and optimize them using evolutionary strategies [47, 66]. To promote generalization across subproblems, metalearning techniques are introduced [67]. However, this paradigm suffers from high training overhead and the burden of maintaining multiple models. In contrast, the one-to-many paradigm employs a single neural network to handle all subproblems. This includes hypernetwork-based DRL frameworks that condition on weight vectors [35, 38, 58], and conditional neural heuristics that incorporate instance features, weight information, and problem size [6, 14].

Preference optimization. Preference optimization methods, such as Direct Preference Optimization (DPO) [44] and Identity Preference Optimization (IPO) [2], have gained significant traction, particularly in large language model (LLM) training, due to their ability to directly optimize human preferences without relying on explicit reward modeling as required in reinforcement learning from human feedback (RLHF). These methods are typically designed for pairwise preference data, where human annotators identify a preferred output over a less preferred one in response to a given prompt. Another line of research explores simpler preference optimization objectives that do not depend on a reference model [21, 62]. Among them, SimPO [41] proposes using the average log-probability of a generated sequence as an implicit reward. This approach aligns more closely with the model's generation process and improves computational and memory efficiency by eliminating the need for a separate reference model. Some studies [37] have explored applying preference optimization to SOCOPs, but its application to MOCOPs has been rarely investigated.

3 Preliminary

3.1 MOCOP

An MOCOP instance specified by data \mathcal{G} can be formally defined as $\min_{\pi \in \mathcal{X}} F(\pi) = (f_1(\pi), f_2(\pi), \dots, f_{\kappa}(\pi))$, where F is the objective vector with κ objective functions, π is a feasible solution, and \mathcal{X} denotes the feasible solution space. Due to inherent conflicts among objectives, a single solution that simultaneously optimizes all objectives typically does not exist. Instead, Pareto optimal solutions are sought to represent different trade-offs, often guided by weight vectors, among competing objectives. We define the Pareto properties of the solutions as follows.

Definition 1 (Pareto Dominance). A solution $\pi \in \mathcal{X}$ is said to dominate another solution $\pi' \in \mathcal{X}$ (i.e., $\pi \prec \pi'$) if and only if $f_i(\pi) \leq f_i(\pi')$, $\forall i \in \{1, \dots, \kappa\}$, and $F(\pi) \neq F(\pi')$.

Definition 2 (Pareto Optimality). A solution $\pi^* \in \mathcal{X}$ is Pareto optimal if it is not dominated by any other solution. Accordingly, the Pareto set \mathcal{P} is defined as all Pareto optimal solutions, i.e., $\mathcal{P} = \{\pi^* \in \mathcal{X} | \nexists \pi \in \mathcal{X} : \pi \prec \pi^* \}$. The Pareto front \mathcal{F} is defined as images of Pareto optimal solutions in the objective space, i.e., $\mathcal{F} = \{F(\pi^*) | \pi^* \in \mathcal{P} \}$.

Decomposition-based Methods. Since solving a SOCOP optimally is NP-hard, MOCOPs are significantly more intractable due to the need to identify Pareto optimal solutions, the quantity of which

grows exponentially with the problem size. Therefore, MOEAs are commonly adopted to compute approximate Pareto solutions. Among them, decomposition-based MOEAs (MOEA/Ds) solve a set of subproblems (i.e., SOCOPs) derived from the original MOCOP, a foundation underlying recent DRL-based neural methods. Specifically, the vanilla MOEA/D utilizes decomposition techniques to scalarize an MOCOP into N subproblems with a set of uniformly distributed weight vectors $\{\lambda_1, \lambda_2, \cdots, \lambda_N\}$, each of which satisfies $\lambda_i = (\lambda_i^1, \cdots, \lambda_i^\kappa)^\top$, $\forall \lambda_i^j \geq 0$ and $\sum_{j=1}^\kappa \lambda_i^j = 1$.

3.2 Subproblem Solving

Given a subproblem (\mathcal{G}, λ_i) , we formulate the solving process as a Markov Decision Process (MDP). An *agent* iteratively takes the current *state* as input (e.g., the instance information and the partially constructed solution), and outputs a probability distribution over the nodes to be selected next. An *action* corresponds to selecting a node, either greedily or by sampling from the predicted probabilities. The *transition* involves appending the selected node to the partial solution. We parameterize the *policy* p by a deep neural network θ , such that the probability of constructing a complete solution π is defined as $p_{\theta}(\pi|\mathcal{G}, \lambda_i) = \prod_{t=1}^T p_{\theta}(\pi_t|\pi_{< t}, \mathcal{G}, \lambda_i)$, where T is the total number of steps, and π_t and $\pi_{< t}$ represent the selected node and partial solution at the t-th step, respectively. The *reward* is defined as the negation of the scalarized objective, e.g., $\mathcal{R}(\pi) = -\sum_{j=1}^{\kappa} \lambda_i^j f_j(\pi)$ with weighted sum decomposition. The policy network is typically optimized using the REINFORCE [56], which maximizes the expected reward $\mathcal{L}(\theta|\mathcal{G}, \lambda_i) = \mathbb{E}_{p_{\theta}(\pi|\mathcal{G}, \lambda_i)}\mathcal{R}(\pi)$ via the following gradient estimator:

$$\nabla_{\theta} \mathcal{L}(\theta|\mathcal{G}, \lambda_i) = \mathbb{E}_{p_{\theta}(\pi|\mathcal{G}, \lambda_i)}[(\mathcal{R}(\pi) - b(\mathcal{G}))\nabla_{\theta} \log p_{\theta}(\pi|\mathcal{G}, \lambda_i)], \tag{1}$$

where the baseline function $b(\cdot)$ reduces the gradient variance and stabilizes the training. There are two primary paradigms to extend the above approach to solve MOCOPs. In the *one-to-one* paradigm, methods sequentially train separate models to solve subproblems with a predefined set of weight vectors. However, they often suffer from low training efficiency and generalize poorly to subproblems with unseen weight vectors. In contrast, the *one-to-many* paradigm trains a single model to solve subproblems for arbitrary weight vectors. This is typically achieved by incorporating a subnetwork that transforms each weight vector into model parameters, thus inducing tailored policies for each subproblem. Our POCCO follows the one-to-many paradigm and introduces two key innovations. Specifically, we design a conditional computation block to dynamically route subproblems to different neural architectures, and propose a preference-driven algorithm to train the model effectively.

4 Methodology

4.1 Overview

POCCO is a learning-based framework that trains a portfolio of policies to solve a set of scalarized subproblems $\{(\mathcal{G}, \lambda_i)\}_{i=1}^N$, obtained by decomposing an MOCOP instance. Instead of forcing a single policy to handle all subproblems, which often yields bland and suboptimal behavior, POCCO promotes specialization: each policy is encouraged to focus on a subset of subproblems, yielding a diverse policy ensemble. Such diversity is known to enhance multi-task optimization [53] by expanding the exploration space and ultimately improving solution quality. Technically, we achieve this diversity by activating different subsets of model parameters through a CCO block, enabling distinct computational paths to emerge for different subproblems. Moreover, POCCO should encourage each policy to thoroughly explore the combinatorial solution space during training for reducing suboptimality. To achieve this, we replace raw rewards with preference signals. For each subproblem (\mathcal{G}, λ_i) , we construct a set of winning–losing solution pairs $\{(\pi^{w,j}, \pi^{l,j})\}_{j=1}^K$. Training then proceeds by maximizing the likelihood of the winning solutions while minimizing that of the losing ones, following a BT-style objective. This preference-driven training encourages the learned policy to explore the most promising regions of the search space, leading to more efficient convergence toward higher-quality solutions. Notably, POCCO is a generic, plug-and-play framework that can seamlessly involve different neural solvers for MOCOPs. We demonstrate this by augmenting two SOTA methods, CNH [14] and WE-CA [6], in Section 5.

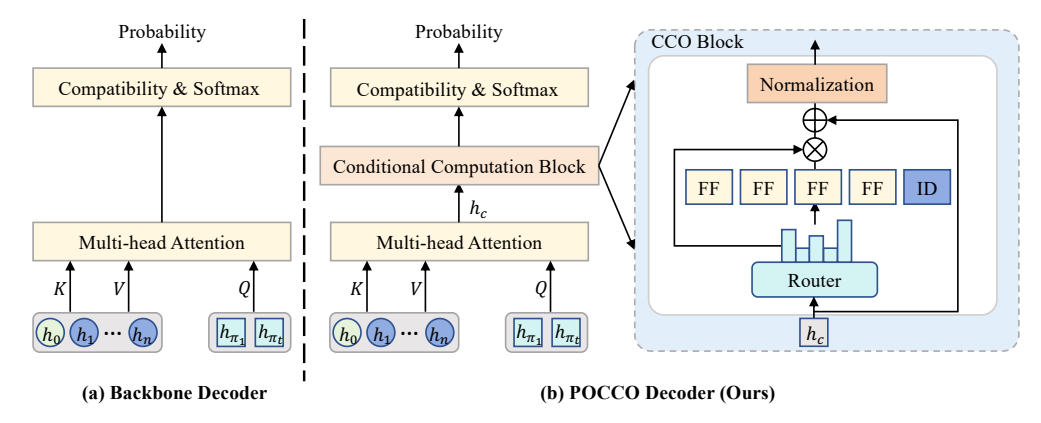


Figure 1: Decoder structures of backbone and POCCO. Given an MOCOP instance $\mathcal G$ with n+1 nodes (e.g., n customers and a depot, if applicable) and a weight vector λ_i , POCCO encodes their raw features into joint node embeddings $\{h_i\}_{i=0}^n$ using an encoder. At each decoding step t, the decoder forms a query Q from the embeddings of the first and last selected nodes (π_1, π_t) , and computes the key K and value V via linear projections of $\{h_i\}_{i=0}^n$. The MHA layer processes Q, K, and V to produce a context vector h_c , which is refined by the CCO block. The refined context is passed through a compatibility layer followed by a Softmax to compute the node selection probabilities. More details about the forward pass can be found in Appendix C.

4.2 Conditional Computational Block

Most approaches employ a Transformer-based architecture, where the encoder generates joint node embeddings $\{h_i\}_{i=0}^n$ that capture the interaction between the instance $\mathcal G$ and the weight vector λ_i , and the decoder produces candidate solutions conditioned on these embeddings. We propose a CCO block to increase the model capacity and promote policy diversity across subproblems. To maintain efficiency, we integrate the CCO block solely into the decoder of the backbone model. This design enables the generation of multiple diverse solutions through a single, computationally expensive encoder pass, offering a favorable trade-off between empirical performance and computational cost.

As illustrated in Fig. 1, the CCO block comprises multiple FF experts and a single ID expert. We insert this block between the multi-head attention (MHA) layer and the compatibility layer in the decoder. Given a batch of MHA outputs $\{h_c^b\}_{b=1}^B$, the CCO block dynamically routes each context vector h_c^b from the corresponding subproblem through either the FF or ID experts, forming distinct computation paths that function as different policies. The ID expert allows the model to bypass the FF computation, promoting architectural sparsity and specialization [19]. Consequently, the CCO block facilitates the learning of dedicated, weight-specific policies tailored to individual subproblems.

Formally, a CCO block consists of: 1) m FF experts $\{E_1, E_2, \ldots, E_m\}$ with independent trainable parameters; 2) a parameter-free identity expert E_{m+1} ; 3) a router, implemented as a gating network G parameterized by W_G , which determines how the inputs $\{h_c^b\}_{b=1}^B$ are routed to the experts; and 4) a skip connection followed by an instance normalization (IN) layer. Given a single context vector h_c^b , let $G(h_c^b) \in \mathbb{R}^{m+1}$ denote the output of the gating network, which represents the expert selection probabilities, and let $E_j(h_c^b)$ denote the output of the j-th expert. The output of the CCO block is:

$$CCO(h_c^b) = IN \left(\sum_{j=1}^{m+1} G(h_c^b)_j E_j(h_c^b) + h_c^b \right).$$
 (2)

The sparse vector $G(h_c^b)$ activates only a small subset of experts, either parameterized FF experts or the parameter-free ID expert, thereby enabling diverse computation paths while reducing computational overhead. A typical implementation uses a $\operatorname{Top} k$ operator that retains the k largest logits and masks the rest with $-\infty$. In this case, the gating network output is: $G(h_c^b) = \operatorname{Softmax}(\operatorname{Top} k(h_c^b \cdot W_G))$.

Our proposed CCO block aligns with the principles of recent advances in efficiently scaling Transformer-based models along both width [48] and depth [45]. In specific, it combines a mixture-of-experts (MoE) layer, implemented using multiple FF experts to widen the network, with a mixture-of-depths (MoD) layer, realized through an ID expert that allows inputs to skip computation. Within the CCO block, each subproblem is adaptively routed to only a small subset of experts,

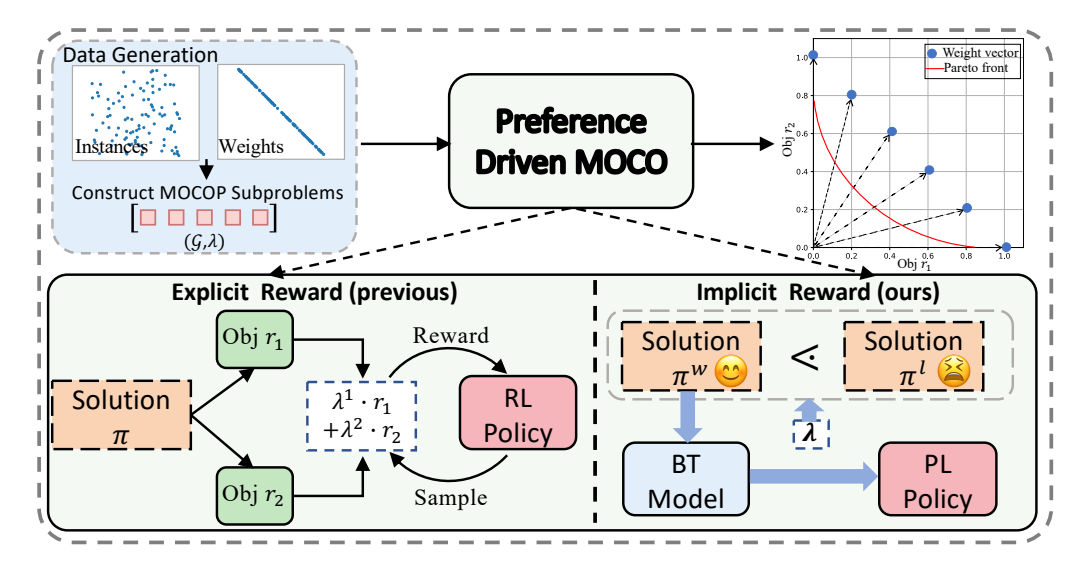


Figure 2: An overview of preference-driven MOCO. Unlike prior DRL methods that explicitly learn from scalarized rewards, our approach converts relative preferences into a BT likelihood, providing an implicit reward signal to optimize the PL policy.

granting the model the expressiveness of a significantly wider network while preserving computational efficiency. As demonstrated in Section 5, this joint design achieves a better capacity–efficiency trade-off than scaling either dimension in isolation.

4.3 Preference-driven MOCO

To mitigate the exploration inefficiencies inherent in REINFORCE algorithms, we optimize *relative preferences* [41] instead of absolute objective values. We summarize our preference-driven MOCO in Appendix D and outline the complete pipeline in Fig. 2, which proceeds in three steps as follows.

Generating preference pairs. For each scalarized subproblem (\mathcal{G}, λ_i) in the training batch, the policy p_θ samples two candidate solutions, π^w and π^l . We denote $\pi^w < \pi^l$ if π^w is preferred over π^l , as determined by the ordering of their scalarized objective values. This evaluator ranks the two solutions and designates the better one as the winning solution π^w and the other as the losing solution π^l . A binary preference label y is then assigned, where y = 1 if $\pi^w < \pi^l$, and y = 0 otherwise. This label serves as the supervision signal required for the preference-driven MOCO.

Defining an implicit reward. Distinct from DRL training paradigms that rely on raw objective values, POCCO treats the average log-likelihood of a solution as an implicit reward f_{θ} , directly relating preferences between solutions to their policy probabilities. This reward is inherently normalized by sequence length $|\pi|$, thereby mitigating length bias between winning and losing solution pairs.

$$f_{\theta}(\pi|\mathcal{G}, \lambda_i) = \frac{1}{|\pi|} \log p_{\theta}(\pi|\mathcal{G}, \lambda_i) = \frac{1}{|\pi|} \sum_{t=1}^{|\pi|} \log p_{\theta}(\pi_t | \pi_{< t}, \mathcal{G}, \lambda_i). \tag{3}$$

Learning from pairwise comparisons. We formulate preference learning (PL) as a probabilistic binary classification problem through the BT model. Specifically, the BT model is a pairwise preference framework that uses a function $g_{\theta}(\cdot)$ to map reward differences into preference probabilities. It assigns each solution a strength proportional to its implicit reward (defined in Eq. (3)) and predicts the probability g_{θ} that the winning solution outranks the losing one:

$$g_{\theta}(\pi^{w} \lessdot \pi^{\ell} \mid \mathcal{G}, \lambda_{i}) = \sigma(\beta \left[f_{\theta}(\pi^{w} \mid \mathcal{G}, \lambda_{i}) - f_{\theta}(\pi^{\ell} \mid \mathcal{G}, \lambda_{i}) \right]), \tag{4}$$

where $\sigma(\cdot)$ is the sigmoid function, and $\beta > 0$ is a fixed temperature that controls the sharpness with which the model distinguishes between unequal rewards. We maximize the likelihood of the collected preferences, yielding the following loss function:

$$\mathcal{L}(\theta|p_{\theta}, \mathcal{G}, \lambda_{i}, \pi^{w}, \pi^{l}) = -y \log \sigma \left(\beta \left[\frac{\log p_{\theta}(\pi^{w}|\mathcal{G}, \lambda_{i})}{|\pi^{w}|} - \frac{\log p_{\theta}(\pi^{l}|\mathcal{G}, \lambda_{i})}{|\pi^{l}|}\right]\right).$$
 (5)

In practice, we collect multiple (π^w, π^ℓ) pairs per update, sum their losses, and backpropagate through p_θ . By maximizing the log-likelihood of $g_\theta(\pi^w \lessdot \pi^\ell \mid \mathcal{G}, \lambda_i)$, the model is encouraged to assign higher probabilities to preferred solutions π^w over less preferred ones π^l .

5 Experiments

5.1 Experimental settings

Training. We conduct extensive experiments to evaluate the effectiveness of the proposed POCCO across various MOCOPs, including multi-objective traveling salesman problem (MOTSP) [39], multi-objective capacitated vehicle routing problem (MOCVRP) [64], and multi-objective knapsack problem (MOKP) [23]. In MOTSP, the goal is to find a tour that visits all nodes exactly once, while minimizing multiple total path lengths, each computed based on a distinct set of coordinates associated with a specific objective. Regarding MOCVRP, a fleet of vehicles with limited capacity must serve all customer nodes and return to the depot, with the objectives of minimizing the total travel distance and the length of the longest individual route. As for MOKP, the problem involves selecting a subset of items, each with a weight and multiple objective-specific values. The objective is to maximize all objective values simultaneously, while ensuring the total weight stays within the knapsack capacity. In this work, we consider three commonly used problem sizes: n = 20/50/100 for MOTSP and MOCVRP, and n = 50/100/200 for MOKP.

Hyperparameters. We implement POCCO on top of two SOTA neural MOCO methods, CNH [14] and WE-CA [6], resulting in POCCO-C and POCCO-W, respectively. Most hyperparameters are aligned with those used in the original CNH and WE-CA implementations. Both models are trained for 200 epochs, with each epoch processing 100,000 randomly sampled instances and a batch size of B=64. We use the Adam optimizer [28] with a learning rate of 3×10^{-4} and a weight decay of 10^{-6} . The N weight vectors used for decomposition are generated following [10], with N=101 for $\kappa=2$ and N=105 for $\kappa=3$.

Baselines. We compare POCCO with a broad range of baseline methods across three categories, all employing weighted-sum (WS) scalarization to ensure fair comparison: (1) Single-model neural MOCO approaches: This includes **PMOCO** [38], and recent SOTA methods **CNH** [14], and WE-CA [6]. Both CNH and WE-CA are unified models trained across problem size $n \in \{20, 21, \cdots, 100\}$ (except $n \in \{50, 51, \cdots, 200\}$ for Bi-KP) (2) Multi-model neural MOCO approaches: This category covers methods like DRL-MOA [34], MDRL [67], and EMNH [7]. Specifically, DRL-MOA trains a separate POMO model for each of the N subproblems, with the first model trained for 200 epochs and the rest fine-tuned for 5 epochs each using parameter transfer. MDRL and EMNH both initialize from a shared pretrained meta-model and fine-tune N subproblemspecific models using the same network structure and training settings as in [7]. (3) Non-learnable approaches, including classical MOEAs and other problem-specific heuristics: MOEA/D [65] and NSGA-II [12], each run for 4,000 iterations, serve as representative decomposition-based and dominance-based MOEAs, respectively. MOCOP-specific MOEAs such as MOGLS [24], configured with 4,000 iterations and 100 local search steps per iteration, and PPLS/D-C [49], run for 200 iterations, are also considered. These methods use 2-opt heuristics for MOTSP and MOCVRP, and a greedy transformation heuristic [23] for MOKP. Finally, WS-LKH and WS-DP combine weighted-sum scalarization with powerful solvers, with LKH [20, 51] used for MOTSP and dynamic programming applied to MOKP.

Inference. We evaluate all methods using three metrics: average hypervolume (HV) [54], average gap, and total runtime per instance set. HV is a widely used indicator in multi-objective optimization that reflects both the convergence and diversity of the solution set. A higher HV indicates better performance. To ensure consistency, HV values are normalized to the range [0, 1] using the same reference point for all methods. The gap is defined as the relative difference between a method's HV and the HV of POCCO-W. Methods with the "-Aug" suffix apply instance augmentation [38] to further improve performance. To evaluate statistical significance, we use the Wilcoxon rank-sum test [55] at a 1% significance level. The best results and others that are not significantly worse are marked in bold, while the second-best and statistically similar results are underlined. All experiments are implemented in Python and conducted on a machine with NVIDIA Ampere A100-80GB GPUs and an AMD EPYC 7742 CPU. The code and dataset are publicly released for reproducibility.²

²https://github.com/mingfan321/POCCO

Table 1: Performance on BiTSP and MOCVRP Instances

Table 1: Performance on BiTSP and MOCVRP Instances									
	1	Bi-TSP20		1	Bi-TSP50		Bi-TSP100		
Method	HV	Gap	Time	HV	Gap	Time	HV	Gap	Time
WS-LKH	0.6270	0.00%	10m	0.6415	0.05%	1.8h	0.7090	-0.17%	6h
MOEA/D	0.6241	0.46%	1.7h	0.6316	1.59%	1.8h	0.6899	2.53%	2.2h
NSGA-II	0.6258	0.19%	6.0h	0.6120	4.64%	6.1h	0.6692	5.45%	6.9h
MOGLS	0.6279	-0.14%	1.6h	0.6330	1.37%	3.7h	0.6854	3.16%	11h
PPLS/D-C	0.6256	0.22%	26m	0.6282	2.12%	2.8h	0.6844	3.31%	11h
DRL-MOA	0.6257	0.21%	6s	0.6360	0.90%	9s	0.6970	1.53%	16s
MDRL	0.6271	-0.02%	5s	0.6364	0.84%	8s	0.6969	1.54%	14s
EMNH	0.6271	-0.02%	5s	0.6364	0.84%	8s	0.6969	1.54%	15s
PMOCO	0.6259	0.18%	6s	0.6351	1.04%	12s	0.6957	1.71%	26s
CNH POCCO-C	$0.6270 \\ 0.6275$	0.00% -0.08%	13s 14s	0.6387 0.6409	$0.48\% \\ 0.14\%$	16s 20s	0.7019 0.7047	$0.83\% \\ 0.44\%$	33s 42s
WE-CA POCCO-W	$0.6270 \\ 0.6275$	$0.00\% \\ -0.08\%$	6s 7s	0.6392 0.6411	$0.41\% \\ 0.11\%$	9s 14s	$0.7034 \\ 0.7055$	$0.62\% \\ 0.32\%$	18s 36s
MDRL-Aug	0.6271	-0.02%	47s	0.6408	0.16%	1.8m	0.7022	0.79%	5.4m
EMNH-Aug	0.6271	-0.02%	46s	0.6408	0.16%	1.8m	0.7023	0.78%	5.4m
PMOCO-Aug	0.6270	0.00%	39s	0.6395	0.36%	1.7m	0.7016	0.88%	5.8m
CNH-Aug	0.6271	-0.02%	1.3m	0.6410	0.12%	3.9m	0.7054	0.34%	12m
POCCO-C-Aug	0.6270	0.00%	2.2m	0.6416	0.03%	4.0m	0.7071	0.10%	14m
WE-CA-Aug	0.6271	-0.02%	1.3m	0.6413	$0.08\% \\ 0.00\%$	3.6m	0.7066	0.17%	12m
POCCO-W-Aug	0.6270	0.00%	2.2m	0.6418		4.0m	<u>0.7078</u>	0.00%	14m
	M	MOCVRP20		MOCVRP50		MO	OCVRP10	0	
Method	HV	Gap	Time	HV	Gap	Time	HV	Gap	Time
MOEA/D	0.4255	1.07%	2.3h	0.4000	2.63%	2.9h	0.3953	3.33%	5.0h
NSGA-II	0.4275	0.60%	6.4h	0.3896	5.16%	8.8h	0.3620	11.47%	9.4h
MOGLS	0.4278	0.53%	9.0h	0.3984	3.02%	20h	0.3875	5.23%	72h
PPLS/D-C	0.4287	0.33%	1.6h	0.4007	2.46%	9.7h	0.3946	3.50%	38h
DRL-MOA	0.4287	0.33%	8s	0.4076	0.78%	12s	0.4055	0.83%	21s
MDRL	0.4291	0.23%	6s	0.4082	0.63%	13s	0.4056	0.81%	22s
EMNH	0.4299	0.05%	7s	0.4098	0.24%	12s	0.4072	0.42%	22s
PMOCO	0.4267	0.79%	6s	0.4036	1.75%	12s	0.3913	4.30%	22s
CNH	0.4287	$0.33\% \\ 0.16\%$	11s	0.4087	0.51%	15s	0.4065	0.59%	25s
POCCO-C	0.4294		16s	0.4101	0.17%	25s	0.4079	0.24%	53s
WE-CA	0.4290	$0.26\% \\ 0.16\%$	7s	0.4089	0.46%	10s	0.4068	0.51%	21s
POCCO-W	0.4294		8s	0.4102	0.15%	17s	0.4084	0.12%	46s
MDRL-Aug	0.4294	0.16%	12s	$\begin{array}{c} 0.4092 \\ \underline{0.4106} \\ 0.4080 \end{array}$	0.39%	36s	0.4072	0.42%	2.8m
EMNH-Aug	0.4302	-0.02%	12s		0.05%	35s	0.4079	0.24%	2.8m
PMOCO-Aug	0.4294	0.16%	14s		0.68%	42s	0.3969	2.93%	2.0m
CNH-Aug	0.4299	0.05%	21s	0.4101	0.17%	45s	0.4077	0.29%	1.9m
POCCO-C-Aug	0.4302	-0.02%	31s	0.4108	0.00%	1.4m	0.4086	0.07%	2.4m
WE-CA-Aug	0.4300	0.02%	15s	0.4103	0.12%	36s	0.4081	0.20%	1.8m
POCCO-W-Aug	<u>0.4301</u>	0.00%	24s	0.4108	0.00%	1.2m	0.4089	0.00%	2.3m

5.2 Experimental results

Comparison analysis. The comparison results are presented in Table 1 and Table 2. POCCO-W consistently achieves superior performance over WE-CA across all benchmark scenarios, establishing itself as the new SOTA results among neural MOCOP solvers. Similarly, POCCO-C outperforms CNH in every case. Both variants also surpass their augmentation-based counterparts, WE-CA-Aug and CNH-Aug, on Bi-TSP20 and Bi-CVRP100, highlighting POCCO's enhanced ability to explore the solution space and approximate high-quality Pareto fronts. When further combined with instance augmentation, POCCO demonstrates additional performance gains. Please note that POCCO with instance augmentation yields lower HV values compared with its non-augmented counterpart on Bi-TSP20. This is because decomposition-based methods focus on optimizing individual subproblems rather than ensuring overall solution diversity. While augmentation improves solution quality for specific subproblems, it may reduce the number of non-dominated solutions, resulting in a smaller HV. Compared with multi-model approaches that require training or fine-tuning separate models for each subproblem, POCCO delivers superior results while maintaining a single shared model. Notably, POCCO achieves better results on Bi-TSP50 than WS-LKH, a setting where previous neural solvers have consistently failed. In terms of efficiency, POCCO significantly reduces computational time.

Table 2: Performance comparison on Bi-KP and Tri-TSP Instances

Method HV Gap Time HV Gap Gas Ga	1	able 2: Pe	errormanc	e comp	arison on	Bi-KP ar	ia Iri-I	SP Instan	ices	
WS-DP 0.3561 0.03% 22m 0.4532 0.04% 2h 0.3601 0.06% 5.8h MOEA/D 0.3540 0.62% 1.6h 0.4508 0.57% 1.7h 0.3581 0.61% 1.8h NSGA-II 0.3540 0.62% 7.8h 0.4520 0.31% 8.0h 0.3590 0.36% 8.4h MOGLS 0.3540 0.62% 5.8h 0.4510 0.53% 10h 0.3582 0.38% 8.4h MOGLS 0.3540 0.62% 5.8h 0.4510 0.53% 10h 0.3582 0.38% 18h PLS/D-C 0.3552 0.98% 8s 0.4531 0.07% 15s 0.3601 0.06% 32s MDRL 0.3530 0.90% 7s 0.4535 -0.02% 17s 0.3601 0.06% 32s EMNH 0.35561 0.03% 7s 0.4535 -0.02% 17s 0.3603 0.00% 4ss POCCO-C 0.3562	Method	В	i-KP50		В	i-KP100		I	3i-KP200	
MOEA/D		HV	Gap	Time	HV	Gap	Time	HV	Gap	Time
NSGA-II	WS-DP	0.3561	0.03%	22m	0.4532	0.04%	2h	0.3601	0.06%	5.8h
MOGLS PPLS/D-C 0.3540 0.62% 0.95% 18m 0.4510 0.53% 10h 0.3582 0.58% 18h 0.4510 0.3528 0.95% 18m 0.4480 1.19% 47m 0.3541 1.72% 1.5h DRL-MOA 0.3559 0.08% 8s 0.4531 0.07% 15s 0.3601 0.06% 32s MDRL 0.3530 0.90% 7s 0.4532 0.04% 18s 0.3601 0.06% 35s EMNH 0.3561 0.03% 7s 0.4535 -0.02% 17s 0.3603 0.00% 48s PMOCO 0.3552 0.28% 8s 0.4535 -0.02% 17s 0.3603 0.00% 48s PMOCCO 0.3550 0.28% 8s 0.4523 0.24% 22s 0.3598 0.14% 55s POCCO-C 0.3560 0.06% 20s 0.4535 -0.02% 36s 0.3603 0.00% 1.4m WE-CA 0.3558 0.11% 8s 0.4527 0.15% 23s 0.3602 0.03% 50s POCCO-W 0.3562 0.00% 11s 0.4534 0.00% 26s 0.3603 0.00% 1.3m MOEA/D 0.4702 0.21% 1.9h 0.4440 -0.07% 1.9h 0.5076 -0.55% 6.6h MOEA/D 0.4702 0.21% 1.9h 0.4440 -0.07% 1.9h 0.5076 -0.55% 6.6h MOGLS 0.4701 0.23% 1.5h 0.4211 5.09% 47.5h 0.2824 44.06% 9.0h MOGLS 0.4701 0.23% 1.5h 0.4211 5.09% 47.5h 0.2824 44.06% 9.0h MOGLS 0.4701 0.23% 1.5h 0.4211 5.09% 47.5h 0.4254 15.73% 13h PPLS/D-C 0.4698 0.30% 1.4h 0.4174 5.93% 3.9h 0.4376 15.31% 14h DRL-MOA 0.4699 0.28% 5s 0.4324 2.55% 10s 0.4852 3.88% 17s EMNH 0.4699 0.28% 5s 0.4321 2.70% 10s 0.4858 3.76% 33s CNH 0.4699 0.28% 5s 0.4321 2.75% 12s 0.4858 3.76% 33s CNH 0.4699 0.28% 5s 0.4321 2.75% 12s 0.4858 3.76% 33s CNH 0.4698 0.30% 1.8h 0.4371 2.70% 10s 0.4856 3.61% 17s PMOCO 0.4698 0.30% 1.8b 0.4335 1.78% 14s 0.4931 2.32% 25s POCCO-C 0.4704 0.17% 18s 0.4393 0.99% 17s 0.4985 1.25% 28s WE-CA 0.4707 0.11% 5s 0.4391 0.09% 13s 0.4956 1.82% 1.5h 0.4711 0.00% 4.2m 0.4408 0.65% 25m 0.4975 1.45% 1.5s 2.88 WE-CA 0.4704 0.17% 18s 0.4397 0.90% 13s 0.4956 1.82% 1.6h PMOCO-Aug 0.4712 0.00% 4.2m 0.4408 0.65% 25m 0.4975 1.45% 1.6h PMOCO-Aug 0.4712 0.00% 4.2m 0.4409 0.63% 28m 0.4956 1.82% 1.6h PMOCO-Aug 0.4704 0.17% 8.5m 0.4409 0.63% 28m 0.4956 1.82% 1.6h PMOCO-Aug 0.4702 0.00% 4.2m 0.4409 0.63% 28m 0.4956 1.82% 1.6h PMOCO-Aug 0.4704 0.17% 8.5m 0.4409 0.63% 28m 0.4996 1.03% 1.6h PMOCO-Aug 0.4712 0.00% 8.2m 0.4409 0.63% 28m 0.4996			0.62%	1.6h	0.4508		1.7h	0.3581	0.61%	
PPLS/D-C	MOGLS			7.011 5.8h	0.4520					18h
MDRL EMNH 0.35501 0.3561 0.90% 0.3687 7s 0.4535 0.4535 -0.02% -0.02% 17s 17s 0.3603 0.00% 48s 48s PMOCO 0.3552 0.28% 8s 0.4523 0.024% 22s 0.3595 0.22% 50s CNH 0.3556 0.17% 16s 0.4527 0.15% 23s 0.3598 0.14% 55s POCCO-C 0.3560 0.06% 20s 0.4535 -0.02% 36s 0.3603 0.00% 1.4m WE-CA 0.3558 0.11% 8s 0.4531 0.07% 16s 0.3602 0.03% 50s POCCO-W 0.3562 0.00% 11s 0.4534 0.00% 26s 0.3602 0.03% 50s POCCO-W 0.3562 0.00% 11s 0.4534 0.00% 26s 0.3602 0.03% 50s POCCO-W 0.3562 0.00% 11s 0.4534 0.00% 16s 0.3602 0.03% 10s 1.3m WE					0.4480	1.19%			1.72%	1.5h
EMNH PMOCO 0.3561 0.03% 0.28% 8s 7s 0.4523 0.24% 22s 0.3505 0.22% 0.22% 50s CNH 0.3556 0.17% 16s 0.4527 0.15% 23s 0.3598 0.3598 0.14% 55s 0.3600 0.06% 20s 0.4535 -0.02% 36s 0.3603 0.00% 1.4m WE-CA 0.3558 0.11% 8s 0.4531 0.07% 16s 0.3602 0.03% 50s 0.3602 0.00% 11s 0.4534 0.00% 12s 0.3603 0.00% 1.3m Method HV Gap Time HV Gap Time WS-LKH 0.4712 0.00% 12m 0.4440 -0.07% 1.9h 0.5076 -0.55% 6.6h MOEA/D 0.4702 0.21% 1.9h 0.4314 2.77% 2.2h 0.4511 10.64% 2.4h NSGA-II 0.4238 10.06% 7.1h 0.2858 35.59% 7.5h 0.2824 44.06% 9.0h MOGLS 0.4701 0.23% 1.5h 0.4211 5.09% 4.1h 0.4254 15.73% 13h PPLS/D-C 0.4698 0.30% 1.4h 0.4174 5.93% 3.9h 0.4376 13.31% 14h DRL-MOA 0.4699 0.28% 6s 0.4303 3.02% 9s 0.4806 4.79% 18s MDRL 0.4699 0.28% 5s 0.4317 2.70% 10s 0.4858 3.76% 33s CNH 0.4698 0.30% 10s 0.4317 2.75% 12s 0.4858 3.76% 33s CNH 0.4698 0.30% 10s 0.4315 2.75% 12s 0.4858 3.76% 33s CNH 0.4698 0.30% 10s 0.4358 1.78% 14s 0.4931 2.32% 2.5s POCCO-C 0.4704 0.17% 18s 0.4393 0.99% 17s 0.4985 1.25% 28s MDRL-Aug 0.4693 0.40% 5s 0.4315 2.75% 12s 0.4858 3.76% 33s CNH 0.4698 0.30% 10s 0.4358 1.78% 14s 0.4931 2.32% 2.5s POCCO-C 0.4704 0.17% 18s 0.4393 0.99% 17s 0.4985 1.25% 23s MDRL-Aug 0.4712 0.00% 4.2m 0.4408 0.65% 25m 0.4975 1.45% 17s POCCO-C 0.4704 0.17% 8.5m 0.4409 0.63% 28m 0.4956 1.03% 1.6h POCCO-C-Aug 0.4712 0.00% 4.2m 0.4408 0.65% 25m 0.4975 1.45% 1.56h POCCO-C-Aug 0.4712 0.		0.3559		<u>8</u> s	0.4531					32s
PMOCO 0.3552 0.28% 8s 0.4523 0.24% 22s 0.3595 0.22% 50s CNH 0.3556 0.17% 16s 0.4527 0.15% 23s 0.3598 0.14% 55s POCCO-C 0.3560 0.06% 20s 0.4535 -0.02% 36s 0.3603 0.00% 1.4m WE-CA 0.3552 0.11% 8s 0.4531 0.07% 16s 0.3602 0.03% 50s POCCO-W 0.3562 0.00% 11s 0.4534 0.00% 26s 0.3603 0.00% 1.3m Method HV Gap Time HV							18s			35s
POCCO-C 0.3560 0.06% 20s 0.4535 -0.02% 36s 0.3603 0.00% 1.4m WE-CA 0.3558 0.11% 8s 0.4531 0.07% 16s 0.3602 0.03% 50s POCCO-W 0.3562 0.00% 11s 0.4534 0.00% 26s 0.3603 0.00% 13m Method HV Gap Time HV Gap Time HV Gap Time WS-LKH 0.4712 0.00% 12m 0.4440 -0.07% 1.9h 0.5076 -0.55% 6.6h MOEA/D 0.4702 0.21% 1.9h 0.4314 2.77% 2.2h 0.4511 10.64% 2.4h NSGA-II 0.4238 10.06% 7.1h 0.2858 35.59% 7.5h 0.2824 44.06% 9.0h MOGLS 0.44701 0.23% 1.5h 0.4211 5.09% 4.1h 0.4254 15.73% 13h PPL-MOCO							22s			
WE-CA POCCO-W 0.3558 0.11% 0.00% 8s 0.4531 0.00% 0.07% 26s 16s 0.3602 0.3603 0.00% 0.00% 0.3603 50s 0.00% 0.3603 Tri-TSP20 Tri-TSP50 Tri-TSP100 Method HV Gap Time Tri-TSP50 Tri-TSP100 WS-LKH 0.4712 0.00% 12m 0.4440 -0.07% 1.9h 0.5076 -0.55% 6.6h MOEA/D 0.4702 0.21% 1.9h 0.4314 2.77% 2.2h 0.4511 10.64% 2.4h 0.406% 7.1h 0.2858 35.59% 7.5h 0.2824 44.06% 9.0h 0.4060GLS 0.4701 0.23% 1.5h 0.4211 5.09% 4.1h 0.4254 15.73% 13h PPLS/D-C 0.4698 0.30% 1.4h 0.4174 5.93% 3.9h 0.4376 13.31% 14h 13h 14h 0.4174 5.93% 3.9h 0.4376 13.31% 14h DRL-MOA 0.4699 0.28% 6s 0.4303 3.02% 9s 0.4806 4.79% 18s 0.4316 0.4699 0.28% 5s 0.4317 2.70% 10s 0.4852 3.88% 17s 0.4699 0.28% 5s 0.4317 2.70% 10s 0.4852 3.88% 17s 0.4699 0.28% 5s 0.4317 2.70% 10s 0.4866 3.61% 17s 0.4699 0.28% 5s 0.4315 2.75% 12s 0.4858 3.76% 33s 0.40% 5s 0.4315 2.75% 12s 0.4858 3.76% 33s 0.40% 5s 0.4315 2.75% 12s 0.4858 3.76% 33s 0.40% 0.4693 0.40% 5s 0.4315 2.75% 12s 0.4858 3.76% 33s 0.4985 1.25% 28s 0.4000 0.4704 0.17% 18s 0.4393 0.99% 17s 0.4985 1.25% 28s 0.4970 0.4704 0.17% 18s 0.4393 0.99% 17s 0.4985 1.25% 23s 0.4985 1.25% 23s 0.4970 0.4710 0.04% 6s 0.4397 0.90% 13s 0.4985 1.25% 23s 0.4973 1.49% 1.6h 0.4000 0.4712 0.00% 4.2m 0.4408 0.65% 25m 0.4973 1.49% 1.6h 0.4000 0.4712 0.00% 4.2m 0.4418 0.43% 25m 0.4996 1.03% 1.6h 0.4000 0.4712 0.00% 4.9m 0.4409 0.63% 28m 0.4996 1.03% 1.6h 0.6000 0.4712 0.00% 4.9m 0.4409 0.63% 28m 0.4996 1.03% 1.6h 0.6000 0.4712 0.00% 4.9m 0.44										55s
POCCO-W 0.3562 0.00% 11s 0.4534 0.00% 26s 0.3603 0.00% 1.3m Method HV Gap Tri-TSP50 Tri-TSP100 WS-LKH 0.4712 0.00% 12m 0.4440 -0.07% 1.9h 0.5076 -0.55% 6.6h MOEA/D 0.4702 0.21% 1.9h 0.4314 2.77% 2.2h 0.4511 10.64% 2.4h NSGA-II 0.4238 10.06% 7.1h 0.2858 35.59% 7.5h 0.2824 44.06% 9.0h MOGLS 0.4701 0.23% 1.5h 0.4211 5.09% 4.1h 0.4254 15.73% 13h PPLS/D-C 0.4698 0.30% 1.4h 0.4174 5.93% 3.9h 0.4376 13.31% 14h DRL-MOA 0.4699 0.28% 5s 0.4317 2.70% 10s 0.4806 3.61% 17s EMNH 0.4699	POCCO-C	0.3560	0.06%	20s	0.4535	-0.02%	36s	0.3603	0.00%	1.4m
Method Tri-TSP20 Tri-TSP50 Tri-TSP100 WS-LKH 0.4712 0.00% 12m 0.4440 -0.07% 1.9h 0.5076 -0.55% 6.6h MOEA/D 0.4702 0.21% 1.9h 0.4314 2.77% 2.2h 0.4511 10.64% 2.4h NSGA-II 0.4238 10.06% 7.1h 0.2858 35.59% 7.5h 0.2824 44.06% 9.0h MOGLS 0.4701 0.23% 1.5h 0.4211 5.09% 4.1h 0.4254 15.73% 13h PPLS/D-C 0.4698 0.30% 1.4h 0.4174 5.93% 3.9h 0.4376 13.31% 14h DRL-MOA 0.4699 0.28% 6s 0.4303 3.02% 9s 0.4806 4.79% 18s MDRL 0.4699 0.28% 5s 0.4317 2.70% 10s 0.4866 3.61% 17s PMOCO 0.4693 0.40% 5s 0.4315 2.75% 10s										
Method HV Gap Time HV Gap Time HV Gap Time WS-LKH 0.4712 0.00% 12m 0.4440 -0.07% 1.9h 0.5076 -0.55% 6.6h MOEA/D 0.4702 0.21% 1.9h 0.4314 2.77% 2.2h 0.4511 10.64% 2.4h NSGA-II 0.4238 10.06% 7.1h 0.2858 35.59% 7.5h 0.2824 44.06% 9.0h MOGLS 0.4701 0.23% 1.5h 0.4211 5.09% 4.1h 0.4254 15.73% 13h PPLS/D-C 0.4698 0.30% 1.4h 0.4174 5.93% 3.9h 0.4376 13.31% 14h DRL-MOA 0.4699 0.28% 5s 0.4317 2.70% 10s 0.4852 3.88% 17s EMNH 0.4699 0.28% 5s 0.4317 2.70% 10s 0.4852 3.88% 17s PMOCO 0.4693	POCCO-W	0.3562								
WS-LKH 0.4712 0.00% 12m 0.4440 -0.07% 1.9h 0.5076 -0.55% 6.6h MOEA/D 0.4702 0.21% 1.9h 0.4314 2.77% 2.2h 0.4511 10.64% 2.4h NSGA-II 0.4238 10.06% 7.1h 0.2858 35.59% 7.5h 0.2824 44.06% 9.0h MOGLS 0.4701 0.23% 1.5h 0.4211 5.09% 4.1h 0.4254 15.73% 13h PPLS/D-C 0.4698 0.30% 1.4h 0.4174 5.93% 3.9h 0.4376 13.31% 14h DRL-MOA 0.4699 0.28% 6s 0.4303 3.02% 9s 0.4806 4.79% 18s MDRL 0.4699 0.28% 5s 0.4317 2.70% 10s 0.4852 3.88% 17s EMNH 0.4699 0.28% 5s 0.4315 2.75% 12s 0.4852 3.88% 17s POCCO-C 0.4704<										
MOEA/D 0.4702 0.21% 1.9h 0.4314 2.77% 2.2h 0.4511 10.64% 2.4h NSGA-II 0.4238 10.06% 7.1h 0.2858 35.59% 7.5h 0.2824 44.06% 9.0h MOGLS 0.4701 0.23% 1.5h 0.4211 5.09% 4.1h 0.4254 15.73% 13h PPLS/D-C 0.4698 0.30% 1.4h 0.4174 5.93% 3.9h 0.4376 13.31% 14h DRL-MOA 0.4699 0.28% 6s 0.4303 3.02% 9s 0.4806 4.79% 18s MDRL 0.4699 0.28% 5s 0.4317 2.70% 10s 0.4852 3.88% 17s EMNH 0.4699 0.28% 5s 0.4315 2.75% 10s 0.4852 3.88% 17s PMOCO 0.4693 0.40% 5s 0.4315 2.75% 12s 0.4858 3.76% 33s CNH 0.4698									-	
NSGA-II 0.4238 10.06% 7.1h 0.2858 35.59% 7.5h 0.2824 44.06% 9.0h MOGLS 0.4701 0.23% 1.5h 0.4211 5.09% 4.1h 0.4254 15.73% 13h PPLS/D-C 0.4698 0.30% 1.4h 0.4174 5.93% 3.9h 0.4376 13.31% 14h DRL-MOA 0.4699 0.28% 6s 0.4303 3.02% 9s 0.4806 4.79% 18s MDRL 0.4699 0.28% 5s 0.4317 2.70% 10s 0.4852 3.88% 17s EMNH 0.4699 0.28% 5s 0.4315 2.75% 10s 0.4866 3.61% 17s PMOCO 0.4693 0.40% 5s 0.4315 2.75% 12s 0.4858 3.76% 33s CNH 0.4698 0.30% 10s 0.4358 1.78% 14s 0.4931 2.32% 25s POCCO-C 0.4704	WS-LKH					-0.07%			-0.55%	
MOGLS 0.4701 0.23% 1.5h 0.4211 5.09% 4.1h 0.4254 15.73% 13h PPLS/D-C 0.4698 0.30% 1.4h 0.4174 5.93% 3.9h 0.4376 13.31% 14h DRL-MOA 0.4699 0.28% 6s 0.4303 3.02% 9s 0.4806 4.79% 18s MDRL 0.4699 0.28% 5s 0.4317 2.70% 10s 0.4852 3.88% 17s EMNH 0.4699 0.28% 5s 0.4315 2.75% 10s 0.4852 3.88% 17s PMOCO 0.4693 0.40% 5s 0.4315 2.75% 12s 0.4858 3.76% 33s CNH 0.4698 0.30% 10s 0.4358 1.78% 14s 0.4931 2.32% 25s POCCO-C 0.4704 0.17% 18s 0.4393 0.99% 17s 0.4985 1.25% 28s WE-CA 0.4710 0.04				1.9h	0.4314	2.77%	2.2h		10.64%	
PPLS/D-C 0.4698 0.30% 1.4h 0.4174 5.93% 3.9h 0.4376 13.31% 14h DRL-MOA 0.4699 0.28% 6s 0.4303 3.02% 9s 0.4806 4.79% 18s MDRL 0.4699 0.28% 5s 0.4317 2.70% 10s 0.4852 3.88% 17s EMNH 0.4699 0.28% 5s 0.4324 2.55% 10s 0.4866 3.61% 17s PMOCO 0.4693 0.40% 5s 0.4315 2.75% 12s 0.4858 3.76% 33s CNH 0.4698 0.30% 10s 0.4358 1.78% 14s 0.4931 2.32% 25s POCCO-C 0.4704 0.17% 18s 0.4393 0.99% 17s 0.4985 1.25% 28s WE-CA 0.4707 0.11% 5s 0.4389 1.08% 8s 0.4975 1.45% 17s POCCO-W 0.4712 0.00% </td <td></td> <td></td> <td>0.06% 0.23%</td> <td>/.In 1.5h</td> <td></td> <td>33.39% 5.09%</td> <td></td> <td></td> <td>44.06% 15.73%</td> <td>9.0n 13h</td>			0.06% 0.23%	/.In 1.5h		33.39% 5.09%			44.06% 15.73%	9.0n 13h
MDRL 0.4699 0.28% 5s 0.4317 2.70% 10s 0.4852 3.88% 17s EMNH 0.4699 0.28% 5s 0.4317 2.70% 10s 0.4866 3.61% 17s PMOCO 0.4693 0.40% 5s 0.4315 2.75% 12s 0.4858 3.76% 33s CNH 0.4698 0.30% 10s 0.4358 1.78% 14s 0.4931 2.32% 25s POCCO-C 0.4704 0.17% 18s 0.4393 0.99% 17s 0.4985 1.25% 28s WE-CA 0.4707 0.11% 5s 0.4389 1.08% 8s 0.4975 1.45% 17s POCCO-W 0.4710 0.04% 6s 0.4397 0.90% 13s 0.4985 1.25% 23s MDRL-Aug 0.4712 0.00% 4.2m 0.4408 0.65% 25m 0.4958 1.78% 1.6h PMOCO-Aug 0.4712 0.00%						5.93%				
PMOCO 0.4693 0.40% 5s 0.4315 2.75% 12s 0.4858 3.76% 33s CNH 0.4698 0.30% 10s 0.4358 1.78% 14s 0.4931 2.32% 25s POCCO-C 0.4704 0.17% 18s 0.4393 0.99% 17s 0.4985 1.25% 28s WE-CA 0.4707 0.11% 5s 0.4389 1.08% 8s 0.4975 1.45% 17s POCCO-W 0.4710 0.04% 6s 0.4397 0.90% 13s 0.4985 1.25% 23s MDRL-Aug 0.4712 0.00% 4.2m 0.4408 0.65% 25m 0.4958 1.78% 1.6h EMNH-Aug 0.4712 0.00% 4.2m 0.4418 0.43% 25m 0.4973 1.49% 1.6h PMOCO-Aug 0.4712 0.00% 4.9m 0.4409 0.63% 28m 0.4956 1.82% 1.6h CNH-Aug 0.4704			0.28%		0.4303			0.4806	4.79%	
PMOCO 0.4693 0.40% 5s 0.4315 2.75% 12s 0.4858 3.76% 33s CNH 0.4698 0.30% 10s 0.4358 1.78% 14s 0.4931 2.32% 25s POCCO-C 0.4704 0.17% 18s 0.4393 0.99% 17s 0.4985 1.25% 28s WE-CA 0.4707 0.11% 5s 0.4389 1.08% 8s 0.4975 1.45% 17s POCCO-W 0.4710 0.04% 6s 0.4397 0.90% 13s 0.4985 1.25% 23s MDRL-Aug 0.4712 0.00% 4.2m 0.4408 0.65% 25m 0.4958 1.78% 1.6h EMNH-Aug 0.4712 0.00% 4.2m 0.4418 0.43% 25m 0.4973 1.49% 1.6h PMOCO-Aug 0.4712 0.00% 4.9m 0.4409 0.63% 28m 0.4956 1.82% 1.6h CNH-Aug 0.4704		0.4699	0.28%	28 58	0.4317	2.70%		0.4852	3.88% 3.61%	1/S 17s
POCCO-C 0.4704 0.17% 18s 0.4393 0.99% 17s 0.4985 1.25% 28s WE-CA 0.4707 0.11% 5s 0.4389 1.08% 8s 0.4975 1.45% 17s POCCO-W 0.4710 0.04% 6s 0.4397 0.90% 13s 0.4985 1.25% 23s MDRL-Aug 0.4712 0.00% 4.2m 0.4408 0.65% 25m 0.4958 1.78% 1.6h EMNH-Aug 0.4712 0.00% 4.2m 0.4418 0.43% 25m 0.4973 1.49% 1.6h PMOCO-Aug 0.4712 0.00% 4.9m 0.4409 0.63% 28m 0.4956 1.82% 1.6h CNH-Aug 0.4704 0.17% 8.5m 0.4409 0.63% 28m 0.4996 1.03% 1.6h POCCO-C-Aug 0.4706 0.13% 8.9m 0.4419 0.41% 34m 0.5023 0.50% 2h WE-CA-Aug 0	PMOCO	0.4693	0.40%	5s	0.4315	2.75%	12s	0.4858	3.76%	33s
WE-CA 0.4707 0.11% 5s 0.4389 1.08% 8s 0.4975 1.45% 17s POCCO-W 0.4710 0.04% 6s 0.4397 0.90% 13s 0.4985 1.25% 23s MDRL-Aug 0.4712 0.00% 4.2m 0.4408 0.65% 25m 0.4958 1.78% 1.6h EMNH-Aug 0.4712 0.00% 4.2m 0.4418 0.43% 25m 0.4973 1.49% 1.6h PMOCO-Aug 0.4712 0.00% 4.9m 0.4409 0.63% 28m 0.4956 1.82% 1.6h CNH-Aug 0.4704 0.17% 8.5m 0.4409 0.63% 28m 0.4996 1.03% 1.6h POCCO-C-Aug 0.4706 0.13% 8.9m 0.4419 0.41% 34m 0.5023 0.50% 2h WE-CA-Aug 0.4712 0.00% 8.2m 0.4432 0.11% 29m 0.5035 0.26% 1.7h	CNH	0.4698	0.30%	10s	0.4358	1.78%	14s	0.4931	2.32%	25s
MDRL-Aug 0.4712 0.00% 4.2m 0.4408 0.65% 25m 0.4958 1.78% 1.6h EMNH-Aug 0.4712 0.00% 4.2m 0.4418 0.43% 25m 0.4973 1.49% 1.6h PMOCO-Aug 0.4712 0.00% 4.9m 0.4409 0.63% 28m 0.4956 1.82% 1.6h CNH-Aug 0.4704 0.17% 8.5m 0.4409 0.63% 28m 0.4996 1.03% 1.6h POCCO-C-Aug 0.4706 0.13% 8.9m 0.4419 0.41% 34m 0.5023 0.50% 2h WE-CA-Aug 0.4712 0.00% 8.2m 0.4432 0.11% 29m 0.5035 0.26% 1.7h										
EMNH-Aug PMOCO-Aug 0.4712 0.4712 0.00% 0.00% 4.2m 4.9m 0.4418 0.4409 0.43% 0.63% 25m 28m 0.4973 0.4956 1.49% 1.82% 1.6h 1.6h CNH-Aug POCCO-C-Aug 0.4704 0.4706 0.17% 0.13% 8.5m 8.9m 0.4409 0.4419 0.63% 0.41% 28m 34m 0.4996 0.5023 1.03% 0.50% 1.6h 2h WE-CA-Aug 0.4712 0.00% 8.2m 0.4432 0.11% 29m 0.5035 0.26% 1.7h	WE-CA POCCO-W			5s 6s	0.4389 0.4397		8s 13s	$0.4975 \\ 0.4985$	1.45% 1.25%	17s 23s
PMOCO-Aug 0.4712 0.00% 4.9m 0.4409 0.63% 28m 0.4956 1.82% 1.6h CNH-Aug 0.4704 0.17% 8.5m 0.4409 0.63% 28m 0.4996 1.03% 1.6h POCCO-C-Aug 0.4706 0.13% 8.9m 0.4419 0.41% 34m 0.5023 0.50% 2h WE-CA-Aug 0.4712 0.00% 8.2m 0.4432 0.11% 29m 0.5035 0.26% 1.7h										
CNH-Aug 0.4704 0.17% 8.5m 0.4409 0.63% 28m 0.4996 1.03% 1.6h POCCO-C-Aug 0.4706 0.13% 8.9m 0.4419 0.41% 34m 0.5023 0.50% 2h WE-CA-Aug 0.4712 0.00% 8.2m 0.4432 0.11% 29m 0.5035 0.26% 1.7h										
POCCO-C-Aug 0.4706 0.13% 8.9m 0.4419 0.41% 34m 0.5023 0.50% 2h WE-CA-Aug 0.4712 0.00% 8.2m 0.4432 0.11% 29m 0.5035 0.26% 1.7h										
WE-CA-Aug 0.4712 0.00% 8.2m 0.4432 0.11% 29m 0.5035 0.26% 1.7h	CNH-Aug	0.4704								
POCCO-W-Aug 0.4712 0.00% 8.9m 0.4437 0.00% 33m 0.5048 0.00% 2h										
		g 0.4712	0.00%							

For example, POCCO-W-Aug solves Bi-TSP100 in only 14 minutes, while WE-LKH requires about 6.0 hours, with POCCO delivering comparable solution quality.

Out-of-distribution size generalization analysis. We evaluate the generalization ability of the models on out-of-distribution, benchmark instances KroAB100/150/200 [40]. All neural methods are trained on Bi-TSP100, except for CNH, WE-CA, and POCCO, which are trained across varying sizes $n \in \{20, 21, \ldots, 100\}$. The results, visualized in Fig. 3, show that POCCO-W-Aug consistently achieves the best generalization performance compared with other neural baselines. POCCO-C-Aug also outperforms CNH-Aug across all evaluated scenarios. Full benchmark results and experiments on larger-scale instances Bi-TSP150/200 are provided in Appendix I and Appendix J, respectively.

Effectiveness of PL. We assess the training efficiency of PL by comparing it to REINFORCE on the WE-CA and POCCO-W models using the Bi-TSP100 dataset. As shown by the validation curves in Fig. 4a, PL achieves faster convergence despite identical network architectures. Notably, for WE-CA, training with PL for 100 epochs reaches performance comparable to 200 epochs of REINFORCE. Similar improvements are observed for POCCO-W. These results demonstrate that PL accelerates the training process and achieves better performance with fewer training epochs.

Effectiveness of the CCO block. To evaluate the impact of the CCO block's structure and placement, we compare POCCO-W with WE-CA and several POCCO variants: POCCO-E (CCO inserted in the encoder replacing the FF layer), POCCO-D (CCO replacing the final linear layer of MHA in the decoder, using MLP experts), POCCO-ME (replacing CCO with a standard MoE layer), POCCO-MD (replacing CCO with three MoD layers), POCCO-MED (using MoE in the encoder and MoD in place of CCO in the decoder), and POCCO-Emp (replacing the identity expert in CCO

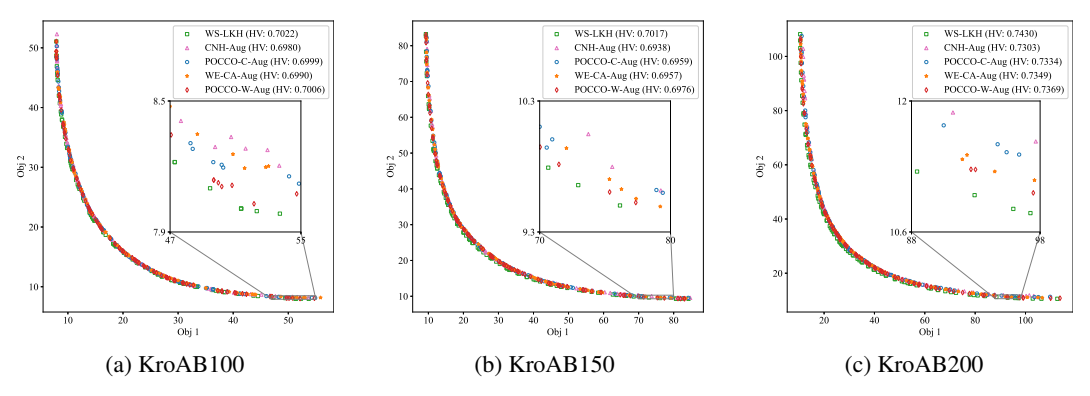


Figure 3: Pareto fronts of benchmark instances.

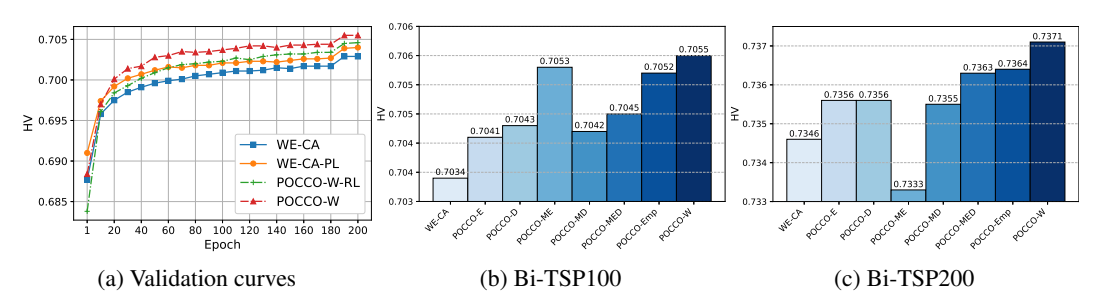


Figure 4: Ablation study:(a) validates the effectiveness of PL; (b) and (c) verify the effects of different CCO block variants.

with an empty expert). As shown in Fig. 4b, all variants outperform WE-CA on the in-distribution Bi-TSP100, with POCCO-W, POCCO-ME, and POCCO-Emp achieving the most notable gains. On the out-of-distribution Bi-TSP200 in Fig. 4c, only POCCO-W and POCCO-Emp maintain strong performance, while POCCO-ME performs worst, even underperforming WE-CA. These results highlight the importance of both the structure and placement of the CCO block for achieving strong generalization across in- and out-of-distribution settings.

Hyperparameter study. We conduct experiments to examine the impact of different key hyperparameters on POCCO's performance. As detailed in Appendix L, the number of CCO block layers, the number of experts, the Top k value, and the temperature parameter β all influence model effectiveness. For the problems studied, the desirable settings, as identified based on empirical results, are: one CCO block layer, four FF experts and one ID expert, Top k = 2, $\beta = 3.5$ for bi-objective tasks, and $\beta = 4.5$ for tri-objective tasks.

6 Conclusion

This paper presents POCCO, a plug-and-play framework tailored for MOCOPs, which adaptively routes subproblems through different model structures and leverages PL for more effective training. POCCO is integrated into two SOTA neural solvers, and extensive experiments demonstrate its effectiveness. Ablation studies further highlight the necessity of both CCO block and PL, and reveal the critical impact of the design and placement of the CCO block. We acknowledge certain limitations, such as the limited capability to address real-world MOCOPs with complex constraints or large problem sizes. Addressing these challenges may require constraint-handling mechanisms [5] or divide-and-conquer [36] strategies, which we leave for future work.

Acknowledgments and Disclosure of Funding

We thank the anonymous reviewers and (S)ACs of NeurIPS 2025 for their constructive comments and dedicated service to the community.

References

- [1] Ehsan Ahmadi, Mostafa Zandieh, Mojtaba Farrokh, and Seyed Mohammad Emami. A multi objective optimization approach for flexible job shop scheduling problem under random machine breakdown by evolutionary algorithms. *Computers & operations research*, 73:56–66, 2016.
- [2] Mohammad Gheshlaghi Azar, Zhaohan Daniel Guo, Bilal Piot, Remi Munos, Mark Rowland, Michal Valko, and Daniele Calandriello. A general theoretical paradigm to understand learning from human preferences. In *International Conference on Artificial Intelligence and Statistics*, pages 4447–4455. PMLR, 2024.
- [3] Irwan Bello, Hieu Pham, Quoc V Le, Mohammad Norouzi, and Samy Bengio. Neural combinatorial optimization with reinforcement learning. In *International Conference on Learning Representations*, 2017.
- [4] Federico Berto, Chuanbo Hua, Junyoung Park, Laurin Luttmann, Yining Ma, Fanchen Bu, Jiarui Wang, Haoran Ye, Minsu Kim, Sanghyeok Choi, Nayeli Gast Zepeda, André Hottung, Jianan Zhou, Jieyi Bi, Yu Hu, Fei Liu, Hyeonah Kim, Jiwoo Son, Haeyeon Kim, Davide Angioni, Wouter Kool, Zhiguang Cao, Qingfu Zhang, Joungho Kim, Jie Zhang, Kijung Shin, Cathy Wu, Sungsoo Ahn, Guojie Song, Changhyun Kwon, Kevin Tierney, Lin Xie, and Jinkyoo Park. RL4CO: an extensive reinforcement learning for combinatorial optimization benchmark. In SIGKDD Conference on Knowledge Discovery and Data Mining, 2025.
- [5] Jieyi Bi, Yining Ma, Jianan Zhou, Wen Song, Zhiguang Cao, Yaoxin Wu, and Jie Zhang. Learning to handle complex constraints for vehicle routing problems. In *Advances in Neural Information Processing* Systems, volume 37, pages 93479–93509, 2024.
- [6] Jinbiao Chen, Zhiguang Cao, Jiahai Wang, Yaoxin Wu, Hanzhang Qin, Zizhen Zhang, and Yue-Jiao Gong. Rethinking neural multi-objective combinatorial optimization via neat weight embedding. In *The Thirteenth International Conference on Learning Representations*, 2025.
- [7] Jinbiao Chen, Jiahai Wang, Zizhen Zhang, Zhiguang Cao, Te Ye, and Siyuan Chen. Efficient meta neural heuristic for multi-objective combinatorial optimization. *Advances in Neural Information Processing Systems*, 36, 2024.
- [8] Xinyun Chen and Yuandong Tian. Learning to perform local rewriting for combinatorial optimization. In International Conference on Neural Information Processing Systems, volume 32, pages 6281–6292, 2019.
- [9] Eng Ung Choo and Derek R Atkins. Proper efficiency in nonconvex multicriteria programming. *Mathematics of Operations Research*, 8(3):467–470, 1983.
- [10] I Das and JE Dennis. Normal-boundary intersection: A new method for generating pareto-optimal points in multieriteria optimization problems. *SIAM J. Optimiz*, 1996.
- [11] Kalyanmoy Deb and Himanshu Jain. An evolutionary many-objective optimization algorithm using reference-point-based nondominated sorting approach, part i: solving problems with box constraints. *IEEE transactions on evolutionary computation*, 18(4):577–601, 2013.
- [12] Kalyanmoy Deb, Amrit Pratap, Sameer Agarwal, and TAMT Meyarivan. A fast and elitist multiobjective genetic algorithm: NSGA-II. IEEE Transactions on Evolutionary Computation, 6(2):182–197, 2002.
- [13] Matthias Ehrgott. Multicriteria optimization, volume 491. Springer Science & Business Media, 2005.
- [14] Mingfeng Fan, Yaoxin Wu, Zhiguang Cao, Wen Song, Guillaume Sartoretti, Huan Liu, and Guohua Wu. Conditional neural heuristic for multiobjective vehicle routing problems. *IEEE Transactions on Neural Networks and Learning Systems*, 2024.
- [15] Wei Fang, Qiang Zhang, Jun Sun, and Xiaojun Wu. Mining high quality patterns using multi-objective evolutionary algorithm. *IEEE Transactions on Knowledge and Data Engineering*, 34(8):3883–3898, 2020.
- [16] Kostas Florios and George Mavrotas. Generation of the exact pareto set in multi-objective traveling salesman and set covering problems. *Applied Mathematics and Computation*, 237:1–19, 2014.
- [17] Keivan Ghoseiri, Ferenc Szidarovszky, and Mohammad Jawad Asgharpour. A multi-objective train scheduling model and solution. *Transportation research part B: Methodological*, 38(10):927–952, 2004.
- [18] Pascal Halffmann, Luca E Schäfer, Kerstin Dächert, Kathrin Klamroth, and Stefan Ruzika. Exact algorithms for multiobjective linear optimization problems with integer variables: A state of the art survey. *Journal of Multi-Criteria Decision Analysis*, 29(5-6):341–363, 2022.

- [19] Jiayi Han, Liang Du, Hongwei Du, Xiangguo Zhou, Yiwen Wu, Weibo Zheng, and Donghong Han. Slim: Let llm learn more and forget less with soft lora and identity mixture. In *North American Chapter of the Association for Computational Linguistics Annual Conference*, 2025.
- [20] Keld Helsgaun. An effective implementation of the lin–kernighan traveling salesman heuristic. *European journal of operational research*, 126(1):106–130, 2000.
- [21] Jiwoo Hong, Noah Lee, and James Thorne. Orpo: Monolithic preference optimization without reference model. In *Proceedings of the 2024 Conference on Empirical Methods in Natural Language Processing*, pages 11170–11189, Miami, Florida, USA, November 2024. Association for Computational Linguistics.
- [22] André Hottung, Yeong-Dae Kwon, and Kevin Tierney. Efficient active search for combinatorial optimization problems. In *International Conference on Learning Representations*, 2021.
- [23] Hisao Ishibuchi, Naoya Akedo, and Yusuke Nojima. Behavior of multiobjective evolutionary algorithms on many-objective knapsack problems. *IEEE Transactions on Evolutionary Computation*, 19(2):264–283, 2014
- [24] Andrzej Jaszkiewicz. Genetic local search for multi-objective combinatorial optimization. *European journal of operational research*, 137(1):50–71, 2002.
- [25] Nicolas Jozefowiez, Frédéric Semet, and El-Ghazali Talbi. Multi-objective vehicle routing problems. European Journal of Operational Research, 189(2):293–309, 2008.
- [26] Liangjun Ke, Qingfu Zhang, and Roberto Battiti. A simple yet efficient multiobjective combinatorial optimization method using decompostion and pareto local search. *IEEE Transactions on Cybernetics*, 44:1808–1820, 2014.
- [27] Minsu Kim, Jinkyoo Park, et al. Learning collaborative policies to solve np-hard routing problems. In International Conference on Neural Information Processing Systems, volume 34, pages 10418–10430, 2021.
- [28] Diederik P Kingma. Adam: A method for stochastic optimization. In *International Conference on Learning Representations*, 2015.
- [29] Wouter Kool, Herke Van Hoof, and Max Welling. Attention, learn to solve routing problems! In *International Conference on Learning Representations*, 2018.
- [30] Yeong-Dae Kwon, Jinho Choo, Byoungjip Kim, Iljoo Yoon, Youngjune Gwon, and Seungjai Min. Pomo: Policy optimization with multiple optima for reinforcement learning. In *International Conference on Neural Information Processing Systems*, volume 33, pages 21188–21198, 2020.
- [31] Philippe Lacomme, Christian Prins, and Marc Sevaux. A genetic algorithm for a bi-objective capacitated arc routing problem. *Computers & Operations Research*, 33(12):3473–3493, 2006.
- [32] Pawel Ladosz, Lilian Weng, Minwoo Kim, and Hyondong Oh. Exploration in deep reinforcement learning: A survey. *Information Fusion*, 85:1–22, 2022.
- [33] Jingwen Li, Yining Ma, Zhiguang Cao, Yaoxin Wu, Wen Song, Jie Zhang, and Yeow Meng Chee. Learning feature embedding refiner for solving vehicle routing problems. *IEEE Transactions on Neural Networks* and Learning Systems, 2023.
- [34] Kaiwen Li, Tao Zhang, and Rui Wang. Deep reinforcement learning for multiobjective optimization. *IEEE Transactions on Cybernetics*, 51(6):3103–3114, 2020.
- [35] Shicheng Li, Feng Wang, Qi He, and Xujie Wang. Deep reinforcement learning for multi-objective combinatorial optimization: A case study on multi-objective traveling salesman problem. Swarm and Evolutionary Computation, page 101398, 2023.
- [36] Sirui Li, Zhongxia Yan, and Cathy Wu. Learning to delegate for large-scale vehicle routing. In *Advances in Neural Information Processing Systems*, volume 34, pages 26198–26211, 2021.
- [37] Zijun Liao, Jinbiao Chen, Debing Wang, Zizhen Zhang, and Jiahai Wang. Bopo: Neural combinatorial optimization via best-anchored and objective-guided preference optimization. In *Proceedings of the 42nd International Conference on Machine Learning (ICML 2025)*, 2025. Poster.
- [38] Xi Lin, Zhiyuan Yang, and Qingfu Zhang. Pareto set learning for neural multi-objective combinatorial optimization. In *International Conference on Learning Representations*, 2022.

- [39] Thibaut Lust and Jacques Teghem. The multiobjective traveling salesman problem: A survey and a new approach. In Advances in Multi-Objective Nature Inspired Computing, pages 119–141. Springer, 2010.
- [40] Thibaut Lust and Jacques Teghem. Two-phase Pareto local search for the biobjective traveling salesman problem. *Journal of Heuristics*, 16(3):475–510, 2010.
- [41] Yu Meng, Mengzhou Xia, and Danqi Chen. Simpo: Simple preference optimization with a reference-free reward. *Advances in Neural Information Processing Systems*, 37:124198–124235, 2024.
- [42] Kaisa Miettinen. Nonlinear multiobjective optimization, volume 12. Springer Science & Business Media, 2012.
- [43] Mohammadreza Nazari, Afshin Oroojlooy, Lawrence Snyder, and Martin Takác. Reinforcement learning for solving the vehicle routing problem. In Advances in Neural Information Processing Systems, volume 31, 2018.
- [44] Rafael Rafailov, Archit Sharma, Eric Mitchell, Christopher D Manning, Stefano Ermon, and Chelsea Finn. Direct preference optimization: Your language model is secretly a reward model. *Advances in Neural Information Processing Systems*, 36:53728–53741, 2023.
- [45] David Raposo, Sam Ritter, Blake Richards, Timothy Lillicrap, Peter Conway Humphreys, and Adam Santoro. Mixture-of-depths: Dynamically allocating compute in transformer-based language models. arXiv preprint arXiv:2404.02258, 2024.
- [46] Haitham Seada and Kalyanmoy Deb. A unified evolutionary optimization procedure for single, multiple, and many objectives. *IEEE Transactions on Evolutionary Computation*, 20(3):358–369, 2015.
- [47] Yinan Shao, Jerry Chun-Wei Lin, Gautam Srivastava, Dongdong Guo, Hongchun Zhang, Hu Yi, and Alireza Jolfaei. Multi-objective neural evolutionary algorithm for combinatorial optimization problems. IEEE Transactions on Neural Networks and Learning Systems, 2021.
- [48] Noam Shazeer, Azalia Mirhoseini, Krzysztof Maziarz, Andy Davis, Quoc Le, Geoffrey Hinton, and Jeff Dean. Outrageously large neural networks: The sparsely-gated mixture-of-experts layer. In *International Conference on Learning Representations*, 2017.
- [49] Jialong Shi, Jianyong Sun, Qingfu Zhang, Haotian Zhang, and Ye Fan. Improving pareto local search using cooperative parallelism strategies for multiobjective combinatorial optimization. *IEEE Transactions on Cybernetics*, 54(4):2369–2382, 2022.
- [50] Ye Tian, Langchun Si, Xingyi Zhang, Ran Cheng, Cheng He, Kay Chen Tan, and Yaochu Jin. Evolutionary large-scale multi-objective optimization: A survey. ACM Computing Surveys, 54(8):1–34, 2021.
- [51] Renato Tinós, Keld Helsgaun, and Darrell Whitley. Efficient recombination in the lin-kernighan-helsgaun traveling salesman heuristic. In Parallel Problem Solving from Nature–PPSN XV: 15th International Conference, Coimbra, Portugal, September 8–12, 2018, Proceedings, Part I 15, pages 95–107. Springer, 2018
- [52] Oriol Vinyals, Meire Fortunato, and Navdeep Jaitly. Pointer networks. In Advances in Neural Information Processing Systems, volume 28, 2015.
- [53] Lirui Wang, Xinlei Chen, Jialiang Zhao, and Kaiming He. Scaling proprioceptive-visual learning with heterogeneous pre-trained transformers. Advances in Neural Information Processing Systems, 37:124420– 124450, 2024.
- [54] Lyndon While, Philip Hingston, Luigi Barone, and Simon Huband. A faster algorithm for calculating hypervolume. *IEEE Transactions on Evolutionary Computation*, 10(1):29–38, 2006.
- [55] Frank Wilcoxon. Individual comparisons by ranking methods. In *Breakthroughs in statistics: Methodology and distribution*, pages 196–202. Springer, 1992.
- [56] Ronald J Williams. Simple statistical gradient-following algorithms for connectionist reinforcement learning. *Machine learning*, 8(3):229–256, 1992.
- [57] Hong Wu, Jiahai Wang, and Zizhen Zhang. MODRL/D-AM: Multiobjective deep reinforcement learning algorithm using decomposition and attention model for multiobjective optimization. In *International Symposium on Intelligence Computation and Applications*, pages 575–589, 2020.
- [58] Yaoxin Wu, Mingfeng Fan, Zhiguang Cao, Ruobin Gao, Yaqing Hou, and Guillaume Sartoretti. Collaborative deep reinforcement learning for solving multi-objective vehicle routing problems. In 23rd International Conference on Autonomous Agents and Multi-Agent Systems (AAMAS), 2023.

- [59] Yaoxin Wu, Wen Song, Zhiguang Cao, Jie Zhang, Abhishek Gupta, and Mingyan Lin. Graph learning assisted multi-objective integer programming. Advances in Neural Information Processing Systems, 35:17774–17787, 2022.
- [60] Yaoxin Wu, Wen Song, Zhiguang Cao, Jie Zhang, and Andrew Lim. Learning improvement heuristics for solving routing problems. IEEE Transactions on Neural Networks and Learning Systems, 2021.
- [61] Yingbo Xie, Shengxiang Yang, Ding Wang, Junfei Qiao, and Baocai Yin. Dynamic transfer reference point-oriented MOEA/D involving local objective-space knowledge. *IEEE Transactions on Evolutionary Computation*, 26(3):542–554, 2022.
- [62] Jing Xu, Andrew Lee, Sainbayar Sukhbaatar, and Jason Weston. Some things are more cringe than others: Preference optimization with the pairwise cringe loss. *arXiv* preprint arXiv:2312.16682, 18, 2023.
- [63] Jiao-Hong Yi, Li-Ning Xing, Gai-Ge Wang, Junyu Dong, Athanasios V Vasilakos, Amir H Alavi, and Ling Wang. Behavior of crossover operators in NSGA-III for large-scale optimization problems. *Information Sciences*, 509:470–487, 2020.
- [64] Sandra Zajac and Sandra Huber. Objectives and methods in multi-objective routing problems: a survey and classification scheme. *European Journal of Operational Research*, 290(1):1–25, 2021.
- [65] Qingfu Zhang and Hui Li. MOEA/D: A multiobjective evolutionary algorithm based on decomposition. *IEEE Transactions on Evolutionary Computation*, 11(6):712–731, 2007.
- [66] Yongxin Zhang, Jiahai Wang, Zizhen Zhang, and Yalan Zhou. MODRL/D-EL: Multiobjective deep reinforcement learning with evolutionary learning for multiobjective optimization. In *International Joint Conference on Neural Networks*, pages 1–8, 2021.
- [67] Zizhen Zhang, Zhiyuan Wu, Hang Zhang, and Jiahai Wang. Meta-learning-based deep reinforcement learning for multiobjective optimization problems. *IEEE Transactions on Neural Networks and Learning Systems*, 2022.
- [68] Aimin Zhou, Qingfu Zhang, and Guixu Zhang. A multiobjective evolutionary algorithm based on decomposition and probability model. In 2012 IEEE Congress on Evolutionary Computation, pages 1–8. IEEE, 2012.
- [69] Jianan Zhou, Zhiguang Cao, Yaoxin Wu, Wen Song, Yining Ma, Jie Zhang, and Xu Chi. MVMoE: Multitask vehicle routing solver with mixture-of-experts. In *International Conference on Machine Learning*, 2024.
- [70] Jianan Zhou, Yaoxin Wu, Wen Song, Zhiguang Cao, and Jie Zhang. Towards omni-generalizable neural methods for vehicle routing problems. In *International Conference on Machine Learning*, 2023.

NeurIPS Paper Checklist

1. Claims

Question: Do the main claims made in the abstract and introduction accurately reflect the paper's contributions and scope?

Answer: [Yes]

Justification: Main contributions and scope are accurately reflect in Abstract and Section 1. Guidelines:

- The answer NA means that the abstract and introduction do not include the claims made in the paper.
- The abstract and/or introduction should clearly state the claims made, including the contributions made in the paper and important assumptions and limitations. A No or NA answer to this question will not be perceived well by the reviewers.
- The claims made should match theoretical and experimental results, and reflect how much the results can be expected to generalize to other settings.
- It is fine to include aspirational goals as motivation as long as it is clear that these goals are not attained by the paper.

2. Limitations

Question: Does the paper discuss the limitations of the work performed by the authors?

Answer: [Yes]

Justification: The limitations are discussed in Section 6.

Guidelines:

- The answer NA means that the paper has no limitation while the answer No means that the paper has limitations, but those are not discussed in the paper.
- The authors are encouraged to create a separate "Limitations" section in their paper.
- The paper should point out any strong assumptions and how robust the results are to violations of these assumptions (e.g., independence assumptions, noiseless settings, model well-specification, asymptotic approximations only holding locally). The authors should reflect on how these assumptions might be violated in practice and what the implications would be.
- The authors should reflect on the scope of the claims made, e.g., if the approach was only tested on a few datasets or with a few runs. In general, empirical results often depend on implicit assumptions, which should be articulated.
- The authors should reflect on the factors that influence the performance of the approach. For example, a facial recognition algorithm may perform poorly when image resolution is low or images are taken in low lighting. Or a speech-to-text system might not be used reliably to provide closed captions for online lectures because it fails to handle technical jargon.
- The authors should discuss the computational efficiency of the proposed algorithms and how they scale with dataset size.
- If applicable, the authors should discuss possible limitations of their approach to address problems of privacy and fairness.
- While the authors might fear that complete honesty about limitations might be used by reviewers as grounds for rejection, a worse outcome might be that reviewers discover limitations that aren't acknowledged in the paper. The authors should use their best judgment and recognize that individual actions in favor of transparency play an important role in developing norms that preserve the integrity of the community. Reviewers will be specifically instructed to not penalize honesty concerning limitations.

3. Theory assumptions and proofs

Question: For each theoretical result, does the paper provide the full set of assumptions and a complete (and correct) proof?

Answer: [NA]

Justification: The paper does not include new theoretical results.

Guidelines:

- The answer NA means that the paper does not include theoretical results.
- All the theorems, formulas, and proofs in the paper should be numbered and cross-referenced.
- All assumptions should be clearly stated or referenced in the statement of any theorems.
- The proofs can either appear in the main paper or the supplemental material, but if they appear in the supplemental material, the authors are encouraged to provide a short proof sketch to provide intuition.
- Inversely, any informal proof provided in the core of the paper should be complemented by formal proofs provided in appendix or supplemental material.
- Theorems and Lemmas that the proof relies upon should be properly referenced.

4. Experimental result reproducibility

Question: Does the paper fully disclose all the information needed to reproduce the main experimental results of the paper to the extent that it affects the main claims and/or conclusions of the paper (regardless of whether the code and data are provided or not)?

Answer: [Yes]

Justification: The paper fully discloses all the information needed to reproduce the main experimental results in Section 5.

Guidelines:

- The answer NA means that the paper does not include experiments.
- If the paper includes experiments, a No answer to this question will not be perceived well by the reviewers: Making the paper reproducible is important, regardless of whether the code and data are provided or not.
- If the contribution is a dataset and/or model, the authors should describe the steps taken to make their results reproducible or verifiable.
- Depending on the contribution, reproducibility can be accomplished in various ways. For example, if the contribution is a novel architecture, describing the architecture fully might suffice, or if the contribution is a specific model and empirical evaluation, it may be necessary to either make it possible for others to replicate the model with the same dataset, or provide access to the model. In general, releasing code and data is often one good way to accomplish this, but reproducibility can also be provided via detailed instructions for how to replicate the results, access to a hosted model (e.g., in the case of a large language model), releasing of a model checkpoint, or other means that are appropriate to the research performed.
- While NeurIPS does not require releasing code, the conference does require all submissions to provide some reasonable avenue for reproducibility, which may depend on the nature of the contribution. For example
- (a) If the contribution is primarily a new algorithm, the paper should make it clear how to reproduce that algorithm.
- (b) If the contribution is primarily a new model architecture, the paper should describe the architecture clearly and fully.
- (c) If the contribution is a new model (e.g., a large language model), then there should either be a way to access this model for reproducing the results or a way to reproduce the model (e.g., with an open-source dataset or instructions for how to construct the dataset).
- (d) We recognize that reproducibility may be tricky in some cases, in which case authors are welcome to describe the particular way they provide for reproducibility. In the case of closed-source models, it may be that access to the model is limited in some way (e.g., to registered users), but it should be possible for other researchers to have some path to reproducing or verifying the results.

5. Open access to data and code

Question: Does the paper provide open access to the data and code, with sufficient instructions to faithfully reproduce the main experimental results, as described in supplemental material?

Answer: [No]

Justification: We promise that the source code and data will be publicly released with the MIT License upon publication.

Guidelines:

- The answer NA means that paper does not include experiments requiring code.
- Please see the NeurIPS code and data submission guidelines (https://nips.cc/public/guides/CodeSubmissionPolicy) for more details.
- While we encourage the release of code and data, we understand that this might not be possible, so "No" is an acceptable answer. Papers cannot be rejected simply for not including code, unless this is central to the contribution (e.g., for a new open-source benchmark).
- The instructions should contain the exact command and environment needed to run to reproduce the results. See the NeurIPS code and data submission guidelines (https://nips.cc/public/guides/CodeSubmissionPolicy) for more details.
- The authors should provide instructions on data access and preparation, including how to access the raw data, preprocessed data, intermediate data, and generated data, etc.
- The authors should provide scripts to reproduce all experimental results for the new
 proposed method and baselines. If only a subset of experiments are reproducible, they
 should state which ones are omitted from the script and why.
- At submission time, to preserve anonymity, the authors should release anonymized versions (if applicable).
- Providing as much information as possible in supplemental material (appended to the paper) is recommended, but including URLs to data and code is permitted.

6. Experimental setting/details

Question: Does the paper specify all the training and test details (e.g., data splits, hyper-parameters, how they were chosen, type of optimizer, etc.) necessary to understand the results?

Answer: [Yes]

Justification: The detailed experimental setups are presented in Section 5.

Guidelines:

- The answer NA means that the paper does not include experiments.
- The experimental setting should be presented in the core of the paper to a level of detail that is necessary to appreciate the results and make sense of them.
- The full details can be provided either with the code, in appendix, or as supplemental material.

7. Experiment statistical significance

Question: Does the paper report error bars suitably and correctly defined or other appropriate information about the statistical significance of the experiments?

Answer: [No]

Justification: Error bars are not reported because it would be too computationally expensive. Guidelines:

- The answer NA means that the paper does not include experiments.
- The authors should answer "Yes" if the results are accompanied by error bars, confidence intervals, or statistical significance tests, at least for the experiments that support the main claims of the paper.
- The factors of variability that the error bars are capturing should be clearly stated (for example, train/test split, initialization, random drawing of some parameter, or overall run with given experimental conditions).
- The method for calculating the error bars should be explained (closed form formula, call to a library function, bootstrap, etc.)
- The assumptions made should be given (e.g., Normally distributed errors).

- It should be clear whether the error bar is the standard deviation or the standard error
 of the mean.
- It is OK to report 1-sigma error bars, but one should state it. The authors should preferably report a 2-sigma error bar than state that they have a 96% CI, if the hypothesis of Normality of errors is not verified.
- For asymmetric distributions, the authors should be careful not to show in tables or figures symmetric error bars that would yield results that are out of range (e.g. negative error rates).
- If error bars are reported in tables or plots, The authors should explain in the text how they were calculated and reference the corresponding figures or tables in the text.

8. Experiments compute resources

Question: For each experiment, does the paper provide sufficient information on the computer resources (type of compute workers, memory, time of execution) needed to reproduce the experiments?

Answer: [Yes]

Justification: Experiments compute resources are indicated in Section 5.

Guidelines:

- The answer NA means that the paper does not include experiments.
- The paper should indicate the type of compute workers CPU or GPU, internal cluster, or cloud provider, including relevant memory and storage.
- The paper should provide the amount of compute required for each of the individual experimental runs as well as estimate the total compute.
- The paper should disclose whether the full research project required more compute than the experiments reported in the paper (e.g., preliminary or failed experiments that didn't make it into the paper).

9. Code of ethics

Question: Does the research conducted in the paper conform, in every respect, with the NeurIPS Code of Ethics https://neurips.cc/public/EthicsGuidelines?

Answer: [Yes]

Justification: This paper respects the NeurIPS Code of Ethics.

Guidelines:

- The answer NA means that the authors have not reviewed the NeurIPS Code of Ethics.
- If the authors answer No, they should explain the special circumstances that require a
 deviation from the Code of Ethics.
- The authors should make sure to preserve anonymity (e.g., if there is a special consideration due to laws or regulations in their jurisdiction).

10. Broader impacts

Question: Does the paper discuss both potential positive societal impacts and negative societal impacts of the work performed?

Answer: [Yes]

Justification: The potential positive societal impacts and negative societal impacts of this work are discussed in Appendix Q.

Guidelines:

- The answer NA means that there is no societal impact of the work performed.
- If the authors answer NA or No, they should explain why their work has no societal impact or why the paper does not address societal impact.
- Examples of negative societal impacts include potential malicious or unintended uses (e.g., disinformation, generating fake profiles, surveillance), fairness considerations (e.g., deployment of technologies that could make decisions that unfairly impact specific groups), privacy considerations, and security considerations.

- The conference expects that many papers will be foundational research and not tied to particular applications, let alone deployments. However, if there is a direct path to any negative applications, the authors should point it out. For example, it is legitimate to point out that an improvement in the quality of generative models could be used to generate deepfakes for disinformation. On the other hand, it is not needed to point out that a generic algorithm for optimizing neural networks could enable people to train models that generate Deepfakes faster.
- The authors should consider possible harms that could arise when the technology is being used as intended and functioning correctly, harms that could arise when the technology is being used as intended but gives incorrect results, and harms following from (intentional or unintentional) misuse of the technology.
- If there are negative societal impacts, the authors could also discuss possible mitigation strategies (e.g., gated release of models, providing defenses in addition to attacks, mechanisms for monitoring misuse, mechanisms to monitor how a system learns from feedback over time, improving the efficiency and accessibility of ML).

11. Safeguards

Question: Does the paper describe safeguards that have been put in place for responsible release of data or models that have a high risk for misuse (e.g., pretrained language models, image generators, or scraped datasets)?

Answer: [NA]

Justification: The paper poses no such risks.

Guidelines:

- The answer NA means that the paper poses no such risks.
- Released models that have a high risk for misuse or dual-use should be released with necessary safeguards to allow for controlled use of the model, for example by requiring that users adhere to usage guidelines or restrictions to access the model or implementing safety filters.
- Datasets that have been scraped from the Internet could pose safety risks. The authors should describe how they avoided releasing unsafe images.
- We recognize that providing effective safeguards is challenging, and many papers do not require this, but we encourage authors to take this into account and make a best faith effort.

12. Licenses for existing assets

Question: Are the creators or original owners of assets (e.g., code, data, models), used in the paper, properly credited and are the license and terms of use explicitly mentioned and properly respected?

Answer: [Yes]

Justification: Licenses for existing assets are detailed in Appendix R.

Guidelines:

- The answer NA means that the paper does not use existing assets.
- The authors should cite the original paper that produced the code package or dataset.
- The authors should state which version of the asset is used and, if possible, include a URL.
- The name of the license (e.g., CC-BY 4.0) should be included for each asset.
- For scraped data from a particular source (e.g., website), the copyright and terms of service of that source should be provided.
- If assets are released, the license, copyright information, and terms of use in the package should be provided. For popular datasets, paperswithcode.com/datasets has curated licenses for some datasets. Their licensing guide can help determine the license of a dataset.
- For existing datasets that are re-packaged, both the original license and the license of the derived asset (if it has changed) should be provided.

• If this information is not available online, the authors are encouraged to reach out to the asset's creators.

13. New assets

Question: Are new assets introduced in the paper well documented and is the documentation provided alongside the assets?

Answer: [NA]

Justification: The paper does not release new assets.

Guidelines:

- The answer NA means that the paper does not release new assets.
- · Researchers should communicate the details of the dataset/code/model as part of their submissions via structured templates. This includes details about training, license, limitations, etc.
- The paper should discuss whether and how consent was obtained from people whose asset is used.
- At submission time, remember to anonymize your assets (if applicable). You can either create an anonymized URL or include an anonymized zip file.

14. Crowdsourcing and research with human subjects

Question: For crowdsourcing experiments and research with human subjects, does the paper include the full text of instructions given to participants and screenshots, if applicable, as well as details about compensation (if any)?

Answer: [NA]

Justification: The paper does not involve crowdsourcing nor research with human subjects. Guidelines:

- The answer NA means that the paper does not involve crowdsourcing nor research with human subjects.
- Including this information in the supplemental material is fine, but if the main contribution of the paper involves human subjects, then as much detail as possible should be included in the main paper.
- According to the NeurIPS Code of Ethics, workers involved in data collection, curation, or other labor should be paid at least the minimum wage in the country of the data collector.

15. Institutional review board (IRB) approvals or equivalent for research with human subjects

Question: Does the paper describe potential risks incurred by study participants, whether such risks were disclosed to the subjects, and whether Institutional Review Board (IRB) approvals (or an equivalent approval/review based on the requirements of your country or institution) were obtained?

Answer: [NA]

Justification: The paper does not involve crowdsourcing nor research with human subjects. Guidelines:

- The answer NA means that the paper does not involve crowdsourcing nor research with human subjects.
- Depending on the country in which research is conducted, IRB approval (or equivalent) may be required for any human subjects research. If you obtained IRB approval, you should clearly state this in the paper.
- We recognize that the procedures for this may vary significantly between institutions and locations, and we expect authors to adhere to the NeurIPS Code of Ethics and the guidelines for their institution.
- · For initial submissions, do not include any information that would break anonymity (if applicable), such as the institution conducting the review.

16. Declaration of LLM usage

Question: Does the paper describe the usage of LLMs if it is an important, original, or non-standard component of the core methods in this research? Note that if the LLM is used only for writing, editing, or formatting purposes and does not impact the core methodology, scientific rigorousness, or originality of the research, declaration is not required.

Answer: [NA]

Justification: The core method development in this research does not involve LLMs as any important, original, or non-standard components.

Guidelines:

- The answer NA means that the core method development in this research does not involve LLMs as any important, original, or non-standard components.
- Please refer to our LLM policy (https://neurips.cc/Conferences/2025/LLM) for what should or should not be described.

Appendix

A Details of MOCOP

Here we elaborate on the problem definitions for the three typical MOCOPs, i.e., MOTSP, MOCVRP, and MOKP.

MOTSP. An MOTSP instance involves multiple cost matrices, aiming to identify a set of tours, i.e., node sequences, that are Pareto optimal. For instance, a κ -objective TSP instance $\mathcal G$ with n+1 nodes is featured by cost matrices $C^i=(c^i_{j,k}),$ with $i\in\{1,\cdots,\kappa\}$ and $j,k\in\{0,\cdots,n\}$. The κ objectives are defined as follows,

$$\min_{\pi \in \mathcal{X}} F(\pi) = \min(f_1(\pi), f_2(\pi), \dots, f_{\kappa}(\pi)),$$
with $f_i(\pi) = c_{\pi_n \pi_0}^i + \sum_{j=0}^{n-1} c_{\pi_j \pi_{j+1}}^i$,
$$(6)$$

where $\pi=(\pi_0,\pi_2,\cdots,\pi_n)$ with $\pi_j\in\{0,\cdots,n\}$. $\mathcal X$ represents all feasible solutions (i.e., tours), ensuring each node is visited exactly once. This paper considers the Euclidean MOTSP following [16, 34, 38]. Each node j has a 2κ -dim feature vector $o_j=[loc_j^1,loc_j^2,\cdots,loc_j^\kappa]$, where $loc_j^i\in\mathbb R^2$ is the coordinate for the i-th objective. The objective $f_i(\pi)$ is defined as $f_i(\pi)=\|loc_{\pi_n}^i-loc_{\pi_0}^i\|_2+\sum_{j=0}^{n-1}\|loc_{\pi_j}^i-loc_{\pi_{j+1}}^i\|_2$.

MOCVRP. An MOCVRP instance consists of n customer nodes and one depot node. Each node has a 3-dim feature vector $o_j = [loc_j, \delta_j]$, where loc_j and δ_j , for $j \in \{0, \cdots, n\}$, correspond to the coordinates and demand of node j. Notably, for the depot node, $o_0 = [loc_0, \delta_0]$, the demand δ_0 is set to 0. Vehicles with a capacity of \mathcal{Q} ($\mathcal{Q} > \delta_i$) are employed to serve all customers in multiple routes, with each route commencing and concluding at the depot. The problem must satisfy the following constraints: 1) Each customer is visited exactly once, and 2) The total demand of customers in each route must not exceed the vehicle's capacity. In our study, we focus on the bi-objective CVRP, aligning with prior research [31, 38]. Specifically, we aim to minimize two objectives: the total length of all routes and the length of the longest route (i.e., the makespan).

MOKP. An MOKP instance consists of n+1 items, where each item j is characterized by a 2-dim feature vector $o_j = [w_j, p_j]$, representing its weight w_j and profit vector p_j , for $j \in \{0, \cdots, n\}$. The profit vector $p_j \in \mathbb{R}^\kappa$ corresponds to κ distinct objective values associated with item j. A knapsack with a capacity of $\mathcal C$ is provided, where $\mathcal C > w_j$ for each item. The goal is to select a subset of items to place into the knapsack while satisfying the following constraint: the total weight of selected items must not exceed the knapsack capacity $\mathcal C$. In our study, we focus on the bi-objective knapsack problem, consistent with previous research [40, 68]. Specifically, we aim to simultaneously maximize two objectives: the sum of the first and second profit components across the selected items.

B Theoretical Analysis

We derive the loss function and gradient for our PL objective and contrast it with the REINFORCE gradient. Our theoretical (and empirical) analyses demonstrate that PL yields significantly lower gradient variance, which contributes to faster and more stable convergence.

B.1 Formulation of Loss Function

Different from the RL, our PL method exploits the preference relations between generated solutions according to their objective. The explicit preference $f^*(\pi|\mathcal{G},\lambda)$ is defined as the negation of the scalarized objective. We contruct a preference pair, denoted as (π^w,π^ℓ) , along with a binary preference label y, where y=1 if $\pi^w < \pi^l$ (i.e., $f^*(\pi^w|\mathcal{G},\lambda) > f^*(\pi^\ell|\mathcal{G},\lambda)$), and y=0 otherwise.

For the policy $p_{\theta}(\pi | \mathcal{G}, \lambda)$ used to construct solution π , its implicit preference is defined as the average log-likelihood: $f_{\theta}(\pi | \mathcal{G}, \lambda) = \frac{1}{|\pi|} \log p_{\theta}(\pi | \mathcal{G}, \lambda)$. For a preference pair (π^w, π^ℓ) , the preference distribution is modeled using the Bradley-Terry (BT) ranking objective and implicit preferences:

$$g_{\theta}(\pi^{w} \lessdot \pi^{\ell} \mid \mathcal{G}, \lambda) = \sigma(\beta \left[f_{\theta}(\pi^{w} \mid \mathcal{G}, \lambda) - f_{\theta}(\pi^{\ell} \mid \mathcal{G}, \lambda) \right]),$$

where $\sigma(\cdot)$ is the sigmoid function, and $\beta>0$ is a fixed temperature that controls the sharpness with which the model distinguishes between unequal rewards. By maximizing the log-likelihood of $g_{\theta}(\pi^w \leqslant \pi^{\ell} \mid \mathcal{G}, \lambda)$, the model is encouraged to assign higher probabilities to preferred solutions π^w compared with less preferred solutions y^{ℓ} . We can derive the PL loss function:

$$\mathcal{L}_{PL}(\theta|p_{\theta}, \mathcal{G}, \lambda, \pi^{w}, \pi^{l}) = -y \log \sigma \left(\beta \left[\frac{\log p_{\theta}(\pi^{w}|\mathcal{G}, \lambda)}{|\pi^{w}|} - \frac{\log p_{\theta}(\pi^{l}|\mathcal{G}, \lambda)}{|\pi^{l}|}\right]\right),$$

PL directly distinguishes optimization signals based on exact preferences, and the strength of the optimization signal correlates with the difference in log-likelihood, requiring the model to maximize the probability gap between π^w and π^ℓ .

B.2 Gradient Analysis

Let z denote the argument of the sigmoid function:

$$z = \beta \left[\frac{\log p_{\theta}(\pi^{w}|\mathcal{G}, \lambda)}{|\pi^{w}|} - \frac{\log p_{\theta}(\pi^{l}|\mathcal{G}, \lambda)}{|\pi^{l}|} \right].$$

The gradient of \mathcal{L}_{PL} with respect to θ is:

$$\nabla_{\theta} \mathcal{L}_{PL} = \frac{\partial \mathcal{L}_{PL}}{\partial z} \cdot \nabla_{\theta} z.$$

Derivative of $-y \log \sigma(z)$ becomes:

$$\frac{\partial \mathcal{L}_{PL}}{\partial z} = -y(1 - \sigma(z)).$$

Gradient of z with respect to θ :

$$\nabla_{\theta} z = \beta \left[\frac{1}{|\pi^w|} \nabla_{\theta} \log p_{\theta}(\pi^w | \mathcal{G}, \lambda) - \frac{1}{|\pi^\ell|} \nabla_{\theta} \log p_{\theta}(\pi^\ell | \mathcal{G}, \lambda) \right].$$

Combining these, the total gradient becomes:

$$\nabla_{\theta} \mathcal{L}_{PL} = -y\beta(1 - \sigma(z)) \left[\frac{1}{|\pi^w|} \nabla_{\theta} \log p_{\theta}(\pi^w | \mathcal{G}, \lambda) - \frac{1}{|\pi^\ell|} \nabla_{\theta} \log p_{\theta}(\pi^\ell | \mathcal{G}, \lambda) \right].$$

The gradient increases the likelihood of π^w and decreases the likelihood of π^ℓ . For comparison, we analyze the loss function in the REINFORCE algorithm here:

$$\mathcal{L}_{BL}(\pi|\mathcal{G},\lambda) = -(\mathcal{R}(\pi) - b)\log p_{\theta}(\pi|\mathcal{G},\lambda),$$

where b is a baseline to distinguish positive or negative optimization signals for each solution π . The gradient of the REINFORCE algorithm is:

$$\nabla_{\theta} \mathcal{L}_{RL} = -(\mathcal{R}(\pi) - b) \nabla_{\theta} \log p_{\theta}(\pi | \mathcal{G}, \lambda).$$

REINFORCE relies on *absolute* returns $\mathcal{R}(\pi)$, whose large variance propagates directly to the gradient. In contrast, \mathcal{L}_{PL} uses *relative* returns inside a sigmoid, yielding the difference of two normalized log-likelihoods. This pairwise, centered signal reduces gradient variance and produces smoother, more stable updates, leading to faster and more reliable convergence. This theoretical insight is further supported by our empirical analyses. We provide concrete evidence of this in Table 3, which reports the average gradient variance in the first five batches of training POCCO-W under both RL and PL frameworks. Across three MOTSP settings, PL consistently exhibits two to four orders of magnitude lower variance, leading to faster convergence and more stable optimization dynamics.

	Table 3: Gradient	variance in	REINFORCE vs.	preference learning.
--	-------------------	-------------	---------------	----------------------

Problem Size	Batch	RL Variance	PL Variance
MOTSP20	1	0.054648	0.000314
	2	0.039951	0.000252
	3	0.019038	0.000191
	4	0.009093	0.000115
	5	0.010742	0.000104
MOTSP50	1	0.474784	0.000142
	2	0.220530	0.000077
	3	0.140275	0.000048
	4	0.092114	0.000040
	5	0.065286	0.000031
MOTSP100	1	10.124832	0.000059
	2	6.355499	0.000039
	3	3.461700	0.000032
	4	1.755804	0.000021
	5	1.111246	0.000014

C MOCOP Solvers with POCCO

Existing neural MOCOP solvers are based on a transformer-based architecture that consists of an encoder and a decoder. The encoder is used to generate embeddings for all nodes based on the instance \mathcal{G} and the weight vector λ . The decoder is used to decode a sequence of actions based on these embeddings in an iterative fashion. To demonstrate the versatility of our POCCO, we integrate it into two SOTA neural methods, WE-CA [6] and CNH [14], yielding POCCO-W and POCCO-C.

C.1 POCCO-W

Given an instance \mathcal{G} comprising n+1 nodes with Z-dimensional features $\{o_i\}_{i=0}^n\subset\mathbb{R}^Z$ and a weight vector λ , first obtains initial embeddings by applying separate linear projections to the node features and the weight vector:

$$h_i^0 = W^o o_i + b^o, \quad \forall i \in \{0, \dots, n\}, \quad h_\lambda^0 = W^\lambda \lambda + b^\lambda,$$
 (7)

where $W^o \in \mathbb{R}^{d \times Z}$, $W^\lambda \in \mathbb{R}^{d \times \kappa}$, and $b^o, b^\lambda \in \mathbb{R}^d$ are learnable parameters, with embedding dimension d=128. POCCO-W integrates the weight embedding into each node embedding in a feature-wise fashion within the encoder. To ensure harmonious interaction, the weight and node embeddings are updated simultaneously. The encoder itself comprises L=6 transformer layers, each layer applying a conditional attention sublayer, followed by a residual Add & Norm (skip connection with instance normalization), a fully connected feed-forward sublayer, and a second Add & Norm.

Specifically, the conditional attention sublayer first conditions node embeddings on the weight embedding via a feature-wise affine transform:

$$\gamma = W^{\gamma} h_{\lambda}^{l-1}, \quad \beta = W^{\beta} h_{\lambda}^{l-1}, \quad h_i' = \gamma \circ h_i^{l-1} + \beta, \quad \forall i \in \{0, \dots, n\},$$
 (8)

where W^{γ} and W^{β} are trainable matrices; \circ denotes element-wise multiplication. Then, the weight and node embeddings are updated via the Multi-Head Attention (MHA) mechanism with 8 heads and an Add & Norm, as follows:

$$\hat{h}_{\lambda} = \operatorname{IN}\left(h_{\lambda}^{l-1} + \operatorname{MHA}\left(h_{\lambda}^{l-1}, \{h_{\lambda}^{l-1}, h_{0}', \dots, h_{n}'\}\right)\right), \tag{9}$$

$$\hat{h}_i = \text{IN}(h_i^{l-1} + \text{MHA}(h_i', \{h_\lambda^{l-1}, h_0', \dots, h_n'\})), \quad \forall i \in \{0, \dots, n\}.$$
(10)

Afterwards, a fully connected feed-forward sublayer and another Add & Norm are employed to yield the weight embedding h^l_λ and the node embeddings $\{h^l_i\}_{i=0}^n$, as follows:

$$h_i^l = \text{IN}(\hat{h}_i + \text{FF}(\hat{h}_i)), \tag{11}$$

$$h_{\lambda}^{l} = \text{IN}(\hat{h}_{\lambda} + \text{FF}(\hat{h}_{\lambda})),$$
 (12)

Given the eventual node embeddings $\{h_i\}_{i=0}^n$ and weight embedding h_λ output by the encoder, the decoder autoregressively computes the probability of node selection over T steps. At decoding step $t \in \{1, \dots, T\}$, the advanced context vector h_c is produced by an MHA layer with 8 heads based on the context embedding v_c and eventual node embeddings as follows:

$$h_c = \text{MHA}\left(v_c, \{h_\lambda, h_0, \dots, h_n\}\right), \tag{13}$$

Context embedding. For MOTSP, the context embedding v_c is obtained by concatenating the embeddings of the first and last visited nodes, and all previously visited nodes are masked when computing selection probabilities. In MOCVRP, v_c consists of the embedding of the last visited node together with the remaining vehicle capacity, while nodes that have already been visited or whose demand exceeds the remaining capacity are masked. In MOKP, the context embedding combines the graph embedding $\bar{h} = \frac{1}{n+1} \sum_{i=0}^n h_i$ with the remaining knapsack capacity, masking both items that are already selected and those whose weight exceeds the remaining capacity when computing selection probabilities.

The context vector h_c is fed through the CCO block to produce a glimpse g_c based on Eq. 2 (i.e., $g_c = \text{CCO}(h_c)$). This glimpse g_c is then used in a compatibility layer to compute unormalized compatibility scores α as follows:

$$\alpha_i = \begin{cases} -\infty, & \text{if node } i \text{ is masked,} \\ C \cdot \tanh\left(\frac{g_c^\top (W^K h_i)}{\sqrt{d}}\right), & \text{otherwise,} \end{cases}$$
 (14)

where C is set to 50 and W^K is a learnable weight matrix. Finally, the node-selection probability for the scalarized subproblem is given by:

$$P_{\theta}(\pi_t \mid \pi_{1:t-1}, s) = \text{Softmax}(\alpha). \tag{15}$$

C.2 POCCO-C

POCCO-C mirrors the overall design of POCCO-W but (i) replaces every conditional-attention sublayer in the encoder with a dual-attention sublayer and (ii) enriches the context vector h_c via a problem-size embedding (PSE) layer. Specifically, each of the L encoder layers in POCCO-C consists of a dual-attention sublayer, followed by a residual Add & Norm, a fully connected feed-forward sublayer, and a second Add & Norm. Concretely, at layer l the dual-attention and first Add & Norm operate as:

$$\hat{h}_{\lambda} = \text{IN}(h_{\lambda}^{l-1} + \text{MHA}(h_{\lambda}^{l-1}, \{h_{\lambda}^{l-1}, h_{0}^{l-1}, \dots, h_{n}^{l-1}\})),$$
(16)

$$\hat{h}_{i}' = \text{MHA}(h_{i}^{l-1}, \{h_{\lambda}^{l-1}, h_{0}^{l-1}, \dots, h_{n}^{l-1}\}) + \text{MHA}(h_{i}^{l-1}, \{h_{\lambda}^{l-1}\}), \quad \forall i \in \{0, \dots, n\}.$$
 (17)

$$\hat{h}_i = \operatorname{IN}(h_i^{l-1} + \hat{h}_i'), \quad \forall i \in \{0, \dots, n\}.$$
(18)

Besides, POCCO-C employs the sinusoidal encoding based on sine and cosine functions to yield the PSE as follows,

$$PSE(\xi, 2i) = sin(\xi/10000^{2i/d}),$$

$$PSE(\xi, 2i + 1) = cos(\xi/10000^{2i/d}),$$
(19)

where $\xi(\xi=n+1)$ and i ($i\in\{0,\cdots,63\}$) mean the problem size and dimension. The resulting d-dimensional PSEs are then processed using two linear layers with trainable matrices $W_{\xi 1}\in\mathbb{R}^{d\times 2d}$ and $W_{\xi 2}\in\mathbb{R}^{2d\times d}$. POCCO-C injects the size information by adding the results from PSE to $\{h_i\}_{i=0}^n$ from the encoder, such that,

$$h_i^{\xi} = h_i + h_{\xi}, \text{ with } h_{\xi} = (PSE(\xi, \cdot)W_{\xi 1})W_{\xi 2}.$$
 (20)

Then, POCCO-C produces the advanced context vector h_c based on the context embedding v_c and the size-injected node embeddings $\{h_i^{\xi}\}_{i=0}^n$ through a MHA layer with 8 heads as follows,

$$h_c = \text{MHA}\left(v_c, \left\{h_0^{\xi}, \dots, h_n^{\xi}\right\}\right). \tag{21}$$

Algorithm 1 Preference-driven MOCO

Input: Instance distribution $\hat{\mathcal{G}}$, weight vector distribution $\hat{\lambda}$, number of training steps E, batch size B, number of tours K per subproblem;

Output: The trained policy network θ ;

- 1: Initialize policy network θ .
- 2: **for** e = 1 to E **do**
- $\lambda_b \sim \text{SampleWeightVector}(\tilde{\lambda}); \mathcal{G}_b \sim \text{SampleInstance}(\tilde{\mathcal{G}}), \quad \forall b \in \{1, \cdots, B\}$
- $\begin{aligned} & \pi^{j,b} \sim \text{SampleSolutions}(p_{\theta}(\cdot|\mathcal{G}_b, \lambda_b)), \, \forall j \in \{1, \cdots, K\} \,, \quad \forall b \in \{1, \cdots, B\} \\ & y^b_{j,p} \sim \text{PairwisePreference}(\mathbf{1}_{[\pi^{j,b} \lessdot \pi^{p,b}]}), \quad \forall j, p \in \{1, \cdots K\}, \, \forall b \in \{1, \cdots, B\} \end{aligned}$ 5:
- Calculate gradient $\nabla_{\theta} \mathcal{L}(\theta)$ according to Eq. (5)
- $\theta \leftarrow \text{ADAM}(\theta, \nabla_{\theta} \mathcal{L}(\theta))$
- 8: end for

Gating Mechanism

Our CCO block employs a subproblem-level gating mechanism to dynamically route each context vector h_c to a subset of experts from a pool consisting of 4 FF experts and 1 ID expert (thus m=4). Let d be the hidden dimension and $W_G \in \mathbb{R}^{d \times (m+1)}$ denote the trainable gating weight matrix. Given a batch of context vectors $X = \{h_c^b\}_{b=1}^B \in \mathbb{R}^{B \times d}$, where B is the batch size, the gating network computes a score matrix: $H = X \cdot W_G \in \mathbb{R}^{B \times (m+1)}$, where each element H_b^j represents the affinity or preference (score) of subproblem b towards expert j.

For each subproblem, the router selects the Top-k highest-scoring experts from the score vector H_h^3 . These selected experts are then activated, and their outputs are weighted by a softmax-normalized version of their scores. In our POCCO with k=2, each subproblem is routed to its two highestscoring experts.

This Top-k routing plays a critical role by reducing computation, as only k experts are activated per subproblem (i.e., sparse activation widely used in MoE structure [69]). It also encourages expert specialization, since different subproblems (defined by context and weight vectors) tend to activate different subsets of experts. Additionally, it allows the inclusion of a parameter-free ID expert, which is often selected when minimal transformation is needed. This enables the router to learn when it is appropriate to leave a representation unchanged.

D **Training Algorithm**

The training algorithm is provided in Algorithm 1. To train the model with preference learning, we first sample a batch of instances and weight vectors $\{(\mathcal{G}_b, \lambda_b)\}_{b=1}^B$ (as in Line 3). Then, for each scalarized subproblem $(\mathcal{G}_b, \lambda_b)$, we construct a set of winning-losing solution pairs $(\pi^{j,b},\pi^{p,b}), \forall j,p \in \{1,\cdots,K\}$ (as in Lines 4-5). Training then proceeds by maximizing the likelihood of the winning solutions while minimizing that of the losing ones (as in Lines 6-7).

\mathbf{E} **Decomposition Approaches**

The major decomposition techniques include weighted-sum, Tchebycheff, and penalty-based boundary intersection (PBI) approaches [42, 65], respectively.

Weighted-sum Approach. Given an MOCOP, the ith subproblem (i.e., SOCOP) is defined with the ith weight vector λ_i , such that,

$$\min \quad g_w(\pi|\lambda_i) = \sum_{j=1}^{\kappa} \lambda_i^j f_j(\pi), \ \pi \in \mathcal{X}$$
 (22)

Tchebycheff Approach. It minimizes the maximal distance between objectives and the ideal reference point, such that,

$$\min \quad g_t(\pi|\lambda_i, z^*) = \max_{1 \le j \le \kappa} \left\{ \lambda_i^j | f_j(\pi) - z_j^* | \right\}, \ \pi \in \mathcal{X}$$
 (23)

where $z^* = (z_1^*, \dots, z_{\kappa}^*)^{\top}$ signifies the ideal reference point with $z_j^* \leq \min\{f_j(\pi) | \pi \in \mathcal{X}\}$. It guarantees that the optimal solution in Eq. (23) under a specific (but unknown) weight vector λ_i could be a Pareto optimal solution [9].

PBI Approach. This approach formulates the *i*th subproblem of an MOCOP as follows,

min
$$g_p(\pi|\lambda) = d_1 + \alpha d_2$$

where $d_1 = \frac{\|(F(\pi) - z^*)^\top \lambda\|}{\|\lambda\|}$
 $d_2 = \|F(\pi) - (z^* + d_1\lambda)\|, \pi \in \mathcal{X}$ (24)

where $\alpha > 0$ is a preset penalty item and z^* is the ideal reference point as defined in the Tchebycheff approach.

F Hypervolume

Hypervolume (HV) is a widely used indicator to evaluate approximate Pareto solutions to MOCOPs. Formally, the HV for a set of solutions \mathcal{P} is defined as the volume of the subspace, which is weakly dominated by the solutions in \mathcal{P} and bounded by a reference point r^* , such that,

$$HV(\mathcal{P}) = \zeta^{\kappa}(\{r \in \mathbb{R}^{\kappa} | \exists \pi \in \mathcal{P}, \pi \prec r \prec r^*\}), \tag{25}$$

where ζ^{κ} denotes the Lebesgue measure on the κ -dimensional space, i.e., the volume for a m-dimensional subspace [54]. Since the range of objective values varies among different problems, we report the normalized HV $\bar{H}(\mathcal{P}) = \mathrm{HV}(\mathcal{P})/\prod_{i=1}^{\kappa}|r_i^*-z_i|$, where the ideal point $z=(z_1,\ldots,z_{\kappa})$ satisfies $z_i < \min\{f_i(\pi) \mid \pi \in \mathcal{P}\}$ (or $z_i > \max\{f_i(\pi) \mid \pi \in \mathcal{P}\}$ for maximization), $\forall i \in \{1,\ldots,\kappa\}$. All methods share the same r^* and z for an MOCOP, as given in Table 4, and we report the average $\bar{H}(\mathcal{P})$ over all test instances in this paper.

Table 4. Ke	rerence	points and ide	ear points.
Problem	Size	r^*	z
	20	(20, 20)	(0,0)
	50	(35, 35)	(0,0)
Bi-TSP	100	(65, 65)	(0, 0)
	150	(85, 85)	(0, 0)
	200	(115, 115)	(0, 0)
	20	(30, 4)	(0,0)
Bi-CVRP	50	(45, 4)	(0,0)
	100	(80, 4)	(0, 0)
	50	(5, 5)	(30, 30)
Bi-KP	100	(20, 20)	(50, 50)
	200	(30, 30)	(75, 75)
	20	(20, 20, 20)	(0,0)
Tri-TSP	50	(35, 35, 35)	(0,0)
	100	(65, 65, 65)	(0, 0)

Table 4: Reference points and ideal points.

G Instance Augmentation

To further improve the performance of POCCO at the inference stage, we apply the instance augmentation proposed in [30], which is also used in PMOCO [38]. The rationale of instance augmentation is that an instance of Euclidean VRPs can be transformed into different ones that share the same optimal solution, e.g., by flipping coordinates for all nodes in an instance. Given a coordinate (x,y) in a VRP, there are eight simple transformations, i.e., (x',y') = (x,y); (y,x); (x,1-y); (y,1-x); (1-x,y); (1-y,x); (1-x,1-y); (1-y,1-x). In our paper, we adopt these transformations for each objective, respectively. Hence, we could have 8 transformations for Bi-CVRP (since there is only one coordinate for each node), $8^2 = 64$ transformations for Bi-TSP, and $8^3 = 512$ transformations for Tri-TSP, respectively.

H Impact of Neutralizing Non-Dominated Pairs

Our method adopts a decomposition-based framework, where the MOCOP is divided into a set of scalarized subproblems, each associated with a weight vector. During training, the goal is to find high-quality solutions with respect to each subproblem, rather than globally exploring the entire Pareto front at once. In this context, preference learning operates at the subproblem level. We acknowledge, however, that sampled solutions may occasionally be mutually non-dominated in the original objective space. To investigate the effect of this scenario, we conducted an additional experiment where preference signals for such non-dominated pairs were set to 0, effectively treating them as equivalent. The results, shown in Table 5, indicate that this modification (NDS) significantly degrades model performance across all Bi-TSP instances.

This observation suggests that introducing indifference signals for non-dominated pairs hinders the learning process. One reason is that it reduces the amount of effective preference supervision per subproblem, especially in early training stages when many solutions are of similar quality. In contrast, using scalarized values provides a consistent and differentiable training signal aligned with the decomposition objective. Therefore, although scalarized comparisons may not reflect global Pareto dominance in every case, they remain well-justified and necessary within the decomposition-based learning paradigm, and do not appear to bias the overall Pareto front approximation based on our empirical findings.

Table 5: Performa	nce on Bi-TSP instance	s when neutralizing	non-dominated pairs.
_			*

Problem Size	POCCO-W HV	NDS HV
Bi-TSP20	0.6275	0.5516
Bi-TSP50	0.6411	0.5160
Bi-TSP100	0.7055	0.5601
Bi-TSP150	0.7033	0.5494
Bi-TSP200	0.7371	0.5809

I Detailed Results on Benchmark Instances

The detailed out-of-distribution generalization results are presented in Table 6, further confirming the exceptional generalization ability of our POCCO.

J Experimental Results on the Larger Problem Sizes

The results on Bi-TSP150/200, summarized in Table 7, show that POCCO-W consistently achieves the best generalization performance compared to all neural baselines and classical MOEAs.

Furthermore, to demonstrate scalability, we include experimental results on even larger problems, including Bi-TSP with 300/500/1000 nodes and MOKP with 300/500/1000 items. These results are summarized in Table 8 and Table 9. As shown, POCCO-W consistently outperforms the baseline WE-CA in most large-scale cases.

K Comparison with DPO

We have added a comparative experiment between our preference learning (PL) method and the recent DPO objective, as shown in Table 10. Since DPO requires two models, i.e., a policy model and a reference model, we use the same architecture and initialization for both, with the reference model updated from the previous epoch. This setup significantly increases training time for DPO (122h vs. 36h for POCCO-W).

As shown in Table 10, while DPO achieves slightly better performance on the smallest instance (MOTSP20), it is consistently outperformed by POCCO-W on larger instances (MOTSP50–200). These results suggest that our PL method offers a more favorable trade-off in terms of both training efficiency and solution quality, especially for large-scale problems.

Table 6: Performance on KroAB Instances

	ŀ	KroAB100		k	KroAB150		ŀ	KroAB200	
Method	HV	Gap	Time	HV	Gap	Time	HV	Gap	Time
WS-LKH	0.7022	-0.23%	2.3m	0.7017	-0.59%	4.0m	0.7430	-0.83%	5.6m
MOEA/D	0.6836	2.43%	5.8m	0.6710	3.81%	7.1m	0.7106	3.57%	7.3m
NSGA-II	0.6676	4.71%	7.0m	0.6552	6.08%	7.9m	0.7011	4.86%	8.4m
MOGLS	0.6817	2.70%	52m	0.6671	4.37%	1.3h	0.7083	3.88%	1.6h
PPLS/D-C	0.6785	3.15%	38m	0.6659	4.54%	1.4h	0.7100	3.65%	3.8h
DRL-MOA	0.6903	1.47%	10s	0.6794	2.61%	12s	0.7185	2.50%	18s
MDRL	0.6881	1.78%	9s	0.6831	2.08%	11s	0.7209	2.17%	16s
EMNH	0.6900	1.51%	9s	0.6832	2.06%	11s	0.7217	2.06%	16s
PMOCO	0.6878	1.83%	9s	0.6819	2.25%	12s	0.7193	2.39%	17s
CNH	0.6947	0.84%	16s	0.6892	1.20%	19s	$0.7250 \\ 0.7302$	1.61%	22s
POCCO-C	0.6965	0.59%	30s	0.6925	0.73%	40s		0.91%	50s
WE-CA	0.6948	0.83%	9s	0.6924	0.75%	12s	0.7317	0.71%	16s
POCCO-W	0.6981	0.36%	20s	0.6946	0.43%	31s	0.7345	0.33%	40s
MDRL-Aug	0.6950	0.80%	10s	0.6890	1.23%	16s	0.7261	1.47%	25s
EMNH-Aug	0.6958	0.69%	10s	0.6892	1.20%	16s	0.7270	1.34%	25s
PMOCO-Aug	0.6937	0.98%	11s	0.6886	1.29%	18s	0.7251	1.60%	30s
CNH-Aug	0.6980	0.37%	17s	0.6938	0.54%	26s	0.7303	0.90%	37s
POCCO-C-Aug	0.6999	0.10%	32s	0.6959	0.24%	48s	0.7334	0.47%	1.1m
WE-CA-Aug	0.6990	0.23%	10s	0.6957	0.27%	20s	0.7349	0.27%	31s
POCCO-W-Aug	0.7006	0.00%	22s	<u>0.6976</u>	0.00%	39s	0.7369	0.00%	59s

Table 7: Performance on Bi-TSP150 and Bi-TSP200 Instances

	E	Bi-TSP150			Bi-TSP200		
Method	HV	Gap	Time	HV	Gap	Time	
WS-LKH	0.7149	-1.23%	13h	0.7490	-1.23%	22h	
MOEA/D	0.6809	3.58%	2.4h	0.7139	3.51%	2.7h	
NSGA-II	0.6659	5.71%	6.8h	0.7045	4.78%	6.9h	
MOGLS	0.6768	4.16%	22h	0.7114	3.85%	38h	
PPLS/D-C	0.6784	3.94%	21h	0.7106	3.96%	32h	
DRL-MOA	0.6901	2.28%	36s	0.7219	2.43%	1.2m	
MDRL	0.6922	1.98%	36s	0.7251	2.00%	1.1m	
EMNH	0.6930	1.87%	37s	0.7260	1.88%	1.1m	
PMOCO	0.6910	2.15%	42s	0.7231	2.27%	1.3m	
CNH	0.6985	1.09%	50s	0.7292	1.45%	1.4m	
POCCO-C	0.7011	0.72%	1.5m	0.7333	0.89%	2.5m	
WE-CA	0.7008	0.76%	45s	0.7346	0.72%	1.3m	
POCCO-W	0.7033	0.41%	1.4m	0.7371	0.38%	2.4m	
MDRL-Aug	0.6976	1.22%	37m	0.7299	1.35%	1.1h	
EMNH-Aug	0.6983	1.12%	39m	0.7307	1.24%	1.1h	
PMOCO-Aug	0.6967	1.35%	40m	0.7283	1.57%	1.2h	
CNH-Aug	0.7025	0.52%	41m	0.7343	0.76%	1.2h	
POCCO-C-Aug	0.7043	0.27%	55m	0.7366	0.45%	1.5h	
WE-CA-Aug	0.7044	0.25%	42m	0.7381	0.24%	1.2h	
POCCO-W-Aug	0.7062	0.00%	45m	0.7399	0.00%	1.4h	

L Hyperparameter Study

Effects of the β . Fig.5 shows how the temperature parameter β in the preference learning loss affects performance (HV) across four benchmark tasks. A moderate value of β consistently yields the best results. For the three bi-objective problems (Bi-TSP100, MOCVRP100, Bi-KP100), performance peaks around $\beta=3.5$; larger or smaller values provide no additional benefit, and in Bi-KP100, an overly large $\beta=5$ sharply degrades HV. For the tri-objective problem (Tri-TSP100), performance improves up to $\beta=4.5$ and then declines slightly. Overall, these trends justify the default settings adopted in our experiments: $\beta=3.5$ for bi-objective tasks and $\beta=4.5$ for tri-objective tasks.

Table 8: HV on large Bi-TSP instances.

Problem Size	WE-CA	POCCO-W
Bi-TSP300	0.7441	0.7458
Bi-TSP500	0.7476	0.7592
Bi-TSP1000	0.7186	0.7400

Table 9: HV on large MOKP instances.

Problem Size	WE-CA	POCCO-W
Bi-KP300	0.6000	0.5947
Bi-KP500	0.4244	0.5658
Bi-KP1000	0.2439	0.8408

Table 10: HV of different PL methods on Bi-TSP instances.

Problem Size	POCCO-W	DPO
Bi-TSP20	0.6275	0.6276
Bi-TSP50	0.6411	0.6400
Bi-TSP100	0.7055	0.7030
Bi-TSP150	0.7033	0.6998
Bi-TSP200	0.7371	0.7331

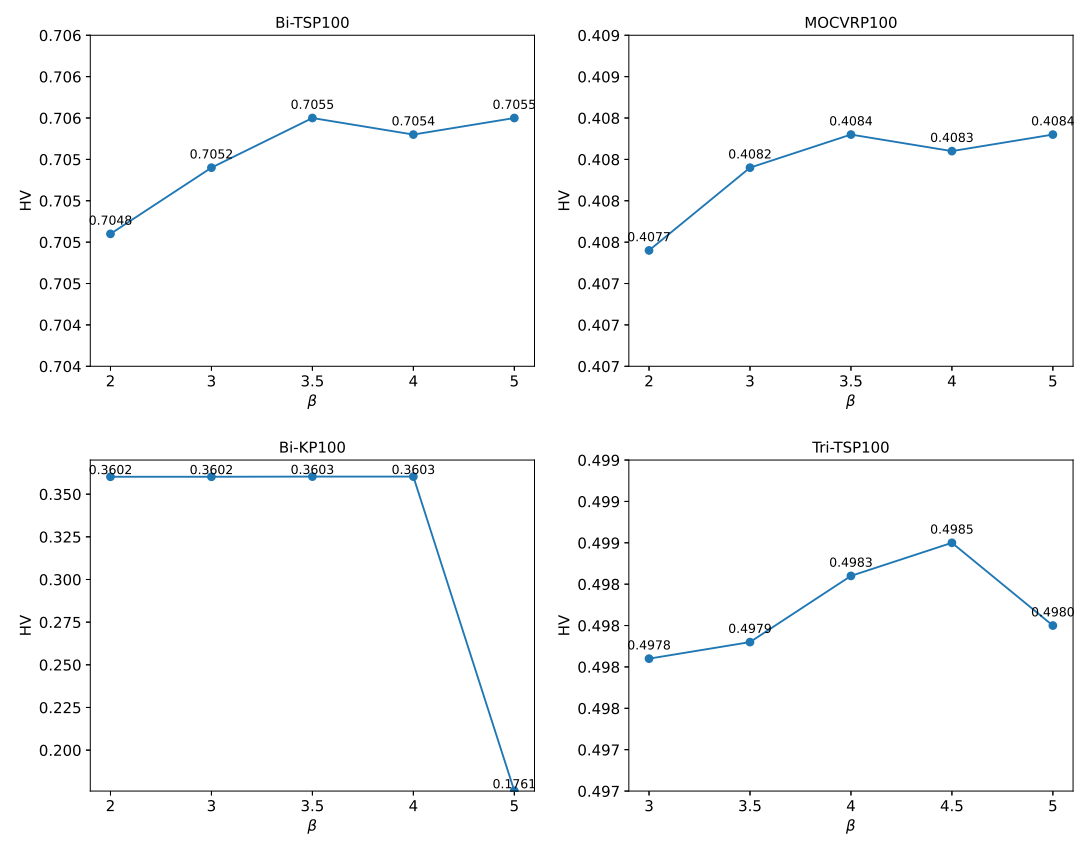


Figure 5: Effectis of the β .

Effects of the number of CCO layers. The CCO block sits in the decoder, whose sequence length T grows with problem size. Each additional CCO layer, therefore, adds a full set of gating and expert computations at every decoding step. Hence, stacking too many CCO layers can inflate the runtime disproportionately. Table 11 reports the trade-off. Using two CCO layers yields the highest HV on both Bi-TSP100 and Bi-TSP200, but increases inference time by roughly 60% and 130 %, respectively. A third layer further slows inference while slightly reducing HV. We therefore adopt a single-layer CCO as the default, which preserves most of the performance gain while keeping computation modest. For larger instances or latency-sensitive applications, the one-layer setting offers a favorable balance between solution quality and speed.

Table 11: Effects of the number of CCO block layers.

	Bi-TS	P100	Bi-TSP200		
Method	HV	Time	HV	Time	
POCCO-W 2 CCO layers 3 CCO layers	0.7055 0.7058 0.7049	36 s 59 s 85 s	0.7371 0.7379 0.7352	2.4 m 5.6 m 7.9 m	

Effects of the number of experts. We have added an ablation study to analyze the impact of the number of experts in Table 12. Specifically, POCCO-W (5E) refers to the original model presented in the paper, which includes 4 feedforward (FF) experts and 1 parameter-free identity (ID) expert. We additionally evaluate four variants:

- 1. POCCO-W (3E): 2 FF + 1 ID;
- 2. POCCO-W (9E): 8 FF + 1 ID;
- 3. POCCO-W (9E 2D): 8 FF + 1 ID, trained on twice the amount of data;
- 4. POCCO-W (17E): 16 FF + 1 ID.

All variants are trained under the same settings as POCCO-W (5E) for a fair comparison, except for POCCO-W (9E 2D), which is trained on more data.

As shown in Table 12, all POCCO-W variants outperform the backbone model WE-CA, confirming the effectiveness of the expert-based architecture. Moreover, POCCO-W (3E) and POCCO-W (5E) achieve better overall performance than POCCO-W (9E) and POCCO-W (17E), the latter of which requires additional data scaling to realize performance gains. To strike a better balance between computational cost and solution quality, we select POCCO-W (5E) as our default model.

Table 12: Effects of the number of experts.

Problem Size	WE-CA	POCCO-W (3E)	POCCO-W (5E)	Exp_num (9E)	Exp_num (9E_2D)	Exp_num (17E)
Bi-TSP20	0.6270	0.6275	0.6275	0.6275	0.6275	0.6275
Bi-TSP50	0.6392	0.6410	0.6411	0.6408	0.6411	0.6408
Bi-TSP100	0.7034	0.7057	0.7055	0.7050	0.7053	0.7050
Bi-TSP150	0.7008	0.7035	0.7033	0.7026	0.7031	0.7027
Bo-TSP200	0.7346	0.7363	0.7371	0.7364	0.7370	0.7361

Effects of Top k. Fig.6 plots validation HV on Bi-TSP100 for $k \in \{1, 2, 3\}$. Selecting two experts per token (k=2) converges fastest and attains the highest final HV. A single expert (k=1) limits model capacity, leading to slower early progress and a slightly lower plateau. Choosing three experts (k=3) increases computation relative to k=2 yet offers no benefit and even marginally reduces HV, likely because the additional expert dilutes specialization and weakens sparsity. We therefore adopt k=2 as the default, balancing performance and efficiency.

M Experimental Results of Scalarized Subproblems

To assess subproblem optimality, we report scalarized objective values for three representative weight vectors $\lambda = (1,0), (0.5,0.5), (0,1)$ on Bi-TSP100 (Table 13). We also compare against single-objective solvers LKH and POMO, each tuned to the corresponding subproblem. Among

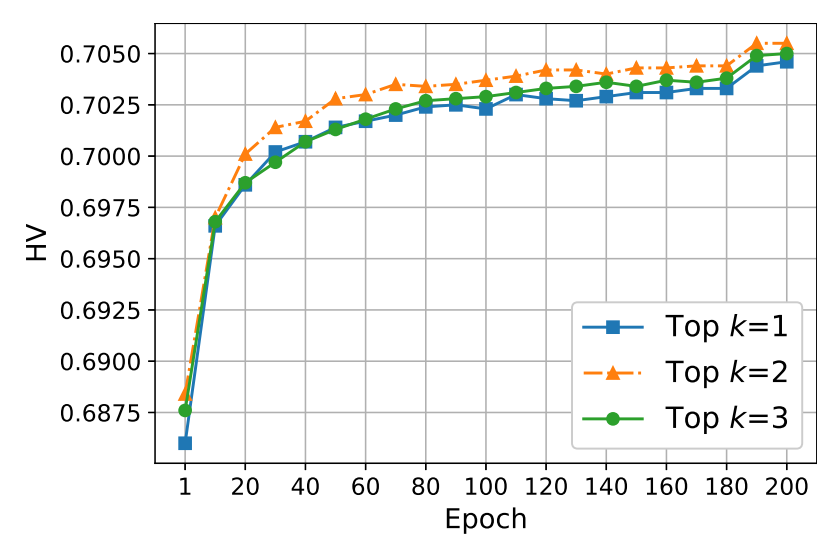


Figure 6: Effects of Top k.

neural MOCOP methods, POCCO-W attains the smallest optimality gaps across all weight settings. Ablating CCO (POCCO-Aug w/o CCO) increases optimality gaps across all settings, and eliminating preference learning as well (WE-CA-Aug) further degrades performance. Notably, POCCO-W-Aug even outperforms POMO-Aug on the subproblem with $\lambda = (0,1)$.

Table 13: Performance comparison under different weight settings (ω_1, ω_2) .

	$\lambda = (1,0)$		$\lambda = (0.5, 0.5)$		$\lambda = (0,1)$	
Method	Obj	Gap	Obj	Gap	Obj	Gap
WS-LKH POMO-Aug WE-CA-Aug POCCO-Aug w/o CCO POCCO-W-Aug	7.7632 7.7659 7.8132 7.7970 7.7827	0.00% 0.03% 0.64% 0.44% 0.25%	17.3094 17.4421 17.4994 17.4629 17.4460	0.00% 0.77% 1.10% 0.89% 0.79%	7.7413 7.7716 7.7888 7.7772 7.7602	0.00% 0.39% 0.61% 0.46% 0.24%

N Comparison with Tchebycheff Scalarization

Intuitively, our POCCO framework is applicable to any MOCOP where the objectives can be scalarized using decomposition-based techniques, including weighted-sum (WS), Tchebycheff (TCH), and penalty-based boundary intersection (PBI). This is because the preference signal between two solutions is determined solely by the ordering of their scalarized objective values, regardless of the specific scalarization method used.

To empirically demonstrate this generality, we added an experiment comparing POCCO-W trained with WS and TCH scalarization methods. As shown in Table 14, WS consistently outperforms TCH on Bi-TSP50 to Bi-TSP200, indicating that WS offers more robust performance across different problem sizes. This observation is also consistent with findings in [6], which report that WS—despite its simplicity—often outperforms TCH in the studied MOCOP setting. In general, however, WE-CA (TCH) performs worse than WE-CA (WS), which achieves a score of 0.6392, and is further outperformed by POCCO-W (TCH), which achieves 0.6395 on Bi-TSP50.

O GPU Memory Usage

We present a comparison of GPU memory usage between POCCO-W (ours), the backbone model (WE-CA), and CNH in Table 15. All models are trained across problem instances with size n=50. As shown in Table 15, POCCO-W incurs higher GPU memory usage, approximately doubling that of

Table 14: HV of Different Decomposition Approaches on Bi-TSP Instances.

Problem Size	WE-CA (WS)	POCCO-W (WS)	POCCO-W (TCH)
Bi-TSP50	0.6392	0.6411	0.6395
Bi-TSP100	0.7034	0.7055	0.7031
Bi-TSP150	0.7008	0.7033	0.6998
Bi-TSP200	0.7346	0.7371	0.7329

Table 15: Comparison of GPU Memory Usage.

Problem Size	WE-CA	CNH	POCCO-W
Bi-TSP50	1051 MB	1077 MB	1849 MB
MOCVRP50	1790 MB	1501 MB	4522 MB
Bi-KP50	916 MB	916 MB	2417 MB
Tri-TSP50	1052 MB	1077 MB	2383 MB

the baselines WE-CA and CNH. However, this increased resource cost is accompanied by significant improvements in solution quality, as demonstrated in our experimental results.

P Summary of Decomposition-based Neural MOCOP Solvers

Table 16 compares key features of decomposition-based neural MOCOP solvers. POCCO, which establishes new SOTA performance, is a plug-and-play framework that augments any existing solver. It inserts a CCO block that learns a diverse ensemble of policies, adding parameters yet surpassing prior methods. Crucially, each subproblem activates only two experts (one of which may be a parameter-free identity expert), so the extra computational load remains minimal. POCCO also employs a pairwise preference learning approach that further boosts performance without introducing additional parameters.

Table 16: Summary of the decomposition-based neural MOCOP solvers.

Method	Learning method	Paradigm	#Parameters
DRL-MOA	Transfer learning+RL	one-to-one	133.37M
MDRL	Meta learning+RL	one-to-one	133.37M
EMNH	Meta learning+RL	one-to-one	133.37M
PMOCO	RL	one-to-many	1.50M
CNH	RL	one-to-many	1.63M
POCCO-C	Preference learning	one-to-many	2.16M
WE-CA	RL	one-to-many	1.47M
POCCO-W	Preference learning	one-to-many	2.00M

Q Broader Impacts

POCCO offers several positive societal impacts. By dynamically routing computation and learning from preference signals, it accelerates multi-objective decision-making in logistics, manufacturing, and energy planning, reducing costly trial-and-error loops and boosting operational efficiency. Its conditional-computation design activates only the required network capacity for each subproblem, cutting FLOP counts and energy consumption relative to dense models of comparable accuracy. Finally, by encouraging exploration and adaptive capacity allocation, POCCO broadens the applicability of neural solvers in complex optimization tasks, advancing both AI and operations research and enabling practitioners to tackle larger, real-world problems with fewer computational resources.

R Licenses for Existing Assets

The used assets in this work are listed in Table 17. Where applicable, we reference publicly available implementations for evaluation or reproduction purposes. Our source code is released under the MIT License.

Table 17: Used assets, licenses, and their usage.

Type	Asset	License	Usage
Code	LKH [20] DRL-MOA [34] MDRL [67] EMNH [7] PMOCO [38] CNH [14] WE-CA [6]	Available for academic use No license (assumed all rights reserved) No license (assumed all rights reserved) No license (assumed all rights reserved) MIT License MIT License MIT License	Evaluation Evaluation Evaluation Evaluation Evaluation Revision Revision
Datasets	Chen et al.[6]	MIT License	Evaluation